Geosci. Model Dev. Discuss., doi:10.5194/gmd-2017-35, 2017
Manuscript under review for journal Geosci. Model Dev.
Discussion started: 17 February 2017

Geoscientific Model Development
Discussions
Open Access

Coupling a three-dimensional subsurface flow and transport model with a land surface model to simulate stream-aquifer-land interactions (PFLOTRAN_CLM v1.0)

Gautam Bisht[1], Maoyi Huang[2,*], Tian Zhou[2], Xingyuan Chen[2], Heng Dai[2], Glenn Hammond[3], William Riley[1], Janelle Downs[2], Ying Liu[2], John Zachara[2]

[1]Lawrence Berkeley National Laboratory, Berkeley, CA

[2]Pacific Northwest National Laboratory, Richland, WA

[3]Sandia National Laboratories, Albuquerque, NM

Correspondence to: Maoyi Huang (maoyi.huang@pnnl.gov)

Geosci. Model Dev. Discuss., doi:10.5194/gmd-2017-35, 2017
Manuscript under review for journal Geosci. Model Dev.
Discussion started: 17 February 2017

Geoscientific Model Development Discussions
Open Access

Abstract

A fully coupled three-dimensional surface and subsurface land model is developed and applied to a site along the Columbia River to simulate three-way interactions among river water, groundwater, and land surface processes. The model features the coupling of the Community Land Model version 4.5 (CLM4.5) and a massively-parallel multi-physics reactive transport model (PFLOTRAN). The coupled model, named PFLOTRAN_CLM v1.0, is applied to a 400 m × 400 m study domain instrumented with groundwater monitoring wells along the Columbia River shoreline. PFLOTRAN_CLM v1.0 simulations are performed at three spatial resolutions over a five-year period to evaluate the impact of hydro-climatic conditions and spatial resolution on simulated variables. Results show that the coupled model is capable of simulating groundwater-river water interactions driven by river stage variability along managed river reaches, which are of global significance as a result of over 30,000 dams constructed worldwide during the past half century. Our numerical experiments suggest that the land-surface energy partitioning is strongly modulated by groundwater-river water interactions through expanding the periodically inundated fraction of the riparian zone, and enhancing moisture availability in the vadose zone via capillary rise in response to the river stage change. Furthermore, spatial resolution is found to impact significantly the accuracy of estimated the mass exchange rates at the boundaries of the aquifer, and it becomes critical when surface and subsurface become more tightly coupled with groundwater table within six to seven meters below the surface. Inclusion of lateral subsurface flow impacted both the surface energy budget and subsurface transport processes. The coupled model developed in this study can be used for improving mechanistic understanding of ecosystem functioning, biogeochemical cycling, and land-atmosphere interactions along river corridors under historical and future hydro-climatic changes. The dataset presented in this study can also serve as a good benchmarking case for testing other integrated models.

Geosci. Model Dev. Discuss., doi:10.5194/gmd-2017-35, 2017
Manuscript under review for journal Geosci. Model Dev.
Discussion started: 17 February 2017

1 Introduction

Previous modeling studies have demonstrated that subsurface hydrologic model structure and parameterization can significantly affect simulated land-atmosphere exchanges [*Condon et al.*, 2013; *Hou et al.*, 2012; *Kollet and Maxwell*, 2008; *Miguez-Macho and Fan*, 2012] and therefore boundary layer dynamics [*Maxwell and Miller*, 2005; *Rihani et al.*, 2015], cloud formation [*Rahman et al.*, 2015], and climate [*Leung et al.*, 2011; *Taylor et al.*, 2013]. Lateral subsurface processes are fundamentally important at multiple spatial scales, including hill-slope scales [*McNamara et al.*, 2005; *Zhang et al.*, 2011], basin scales in semi-arid and arid climates where regional aquifers sustain baseflows in rivers [*Schaller and Fan*, 2009], and wetlands [*Fan and Miguez-Macho*, 2011]. However, some current generation of land surface models (LSMs) routinely omit explicit lateral subsurface processes [*Clark et al.*, 2015; *Kollet and Maxwell*, 2008; *Nir et al.*, 2014], while others include them (described below). Observational and modeling studies suggest that groundwater forms an environmental gradient in soil moisture availability by redistributing water that could profoundly shape critical zone evolution at continental to global scales [*Fan et al.*, 2013; *Taylor et al.*, 2013]. The mismatch between observed and simulated evapotranspiration by current LSMs could be explained by the absence of lateral groundwater flow [*Maxwell and Condon*, 2016].

It has been increasingly recognized that rivers, despite their small aerial extent on the landscape, play important roles in watershed functioning through their connections with groundwater aquifers and riparian zones [*Shen et al.*, 2016]. The interactions between groundwater and river water prolong physical storage and enhance reactive processing that alter water chemistry, downstream transport of materials and energy, and biogenic gas emissions [*Fischer et al.*, 2005; *Harvey and Gooseff*, 2015]. The Earth System modeling community recognizes such a gap in existing ESMs and calls for improved representation of biophysical and biogeochemical processes within the terrestrial-aquatic interface [*Gaillardet et al.*, 2014].

Over the past decade, much effort has been expended to include groundwater into LSMs. Groundwater is important to water and energy budgets such as evapotranspiration (ET), latent heat (LH), and sensible heat (SH), but also to biogeochemical processes such as gross primary production (GPP), heterotrophic respiration (HR), and nutrient cycling. The lateral convergence of water along the landscape and two-way groundwater-surface water exchange are identified as the most relevant subsurface processes to large-scale Earth System functioning (see review by

Geosci. Model Dev. Discuss., doi:10.5194/gmd-2017-35, 2017
Manuscript under review for journal Geosci. Model Dev.
Discussion started: 17 February 2017

Geoscientific Model Development Discussions

Clark et al. [2015]). However, the choice of processes, the approaches to represent multi-scale structures and heterogeneities, the data and computational demands, etc., all vary greatly among the research groups even working on the same land models.

Most of the LSMs reviewed by *Clark et al.* [2015] do not explicitly account fort stream-aquifer-land interactions. For example, the Community Land Model version 4.5 allows for reinfiltration of flooded waters in a highly parameterized way without explicitly linking to groundwater dynamics, therefore only one-way flow from the aquifer to the stream is simulated [*Oleson et al.*, 2013]. The Land-Ecosystem-Atmosphere Feedback (LEAF) model treats river elevation as part of the 2-D vertically integrated groundwater flow equation and allows river and floodwater to infiltrate through sediments in the flood plain [*Miguez-Macho and Fan*, 2012].

In contrast, the fully integrated models, being a small subset of LSMs, explicitly represent the two-way exchange between groundwater aquifers and their adjacent rivers in a spatially resolved fashion. Such models couple a completely integrated hydrology model with a land surface model, so that the surface-water recharge to groundwater by infiltration or intrusion and base flow discharge from groundwater to surface waters can be estimated in a more mechanistic way.

Examples of the fully integrated models include: (1) the coupling between the Common Land Model (CoLM) and a variably saturated groundwater model (ParFlow) [*Maxwell and Miller*, 2005]; (2) the Penn State Integrated Hydrologic Model (PIHM) [*Shi et al.*, 2013]; (3) the coupling between the Process-based Adaptive Watershed Simulator (PAWS) and CLM4.5 [*Ji et al.*, 2015; *Pau et al.*, 2016; *Riley and Shen*, 2014]; and (4) the coupling between the CATchment HYdrology (CATHY) model and the Noah model with multiple parameterization schemes (Noah-MP) [*Niu et al.*, 2014]. The integrated models eliminate the need for parameterizing lateral groundwater flow and allow the interconnected groundwater–surface-water systems to evolve dynamically based on the governing equations and the properties of the physical system. Although such models often require robust numerical solvers on high-performance computing (HPC) facilities to achieve high-resolution, large-extent simulations [*Maxwell et al.*, 2015], they have been increasingly applied for hydrologic prediction and environmental understanding. However, significant discrepancies exist in their simulations when being applied to complex problems due to differences in physical process representations and numerical solution

Geosci. Model Dev. Discuss., doi:10.5194/gmd-2017-35, 2017
Manuscript under review for journal Geosci. Model Dev.
Discussion started: 17 February 2017

approaches, even though many of the models show good agreement for simpler test cases [*Maxwell et al.*, 2014].

We have three aims in this paper. First, we document the development of a fully integrated land surface and subsurface model, featuring the coupling between two highly-scalable and state-of-the-art open-source codes: a reactive transport model PFLOTRAN [*Lichtner et al.*, 2015] and CLM4.5 [*Oleson et al.*, 2013] (PFLOTRAN_CLM v1.0 hereafter), that mechanistically represents the two-way exchange of water and solute mass between aquifers and river as well as land-atmosphere exchange of water and energy. Second, we describe a numerically challenging benchmarking case for verifying fully integrated models, featuring a highly dynamic river boundary condition determined by dam-induced river stage variations, representative of managed river reaches that are of global significance as a result of dam constructions in the past few decades [*Zhou et al.*, 2016]. Third, we assess the effects of spatial resolution and projected hydro-climatic changes on simulated land surface fluxes and exchange of groundwater and river water using the coupled model and datasets from the benchmarking case. In section 2, we describe the component models and our coupling strategy. In section 3, we describe an application of the model to a field site along the Hanford reach of the Columbia River, where the subsurface properties are well characterized and long-term monitoring of river stage, groundwater table, and exchange of groundwater and river water exist. In section 4, we assess the effects of spatial resolution and hydro-climatic conditions to simulated fluxes and state variables. In section 5, conclusion and future work are discussed.

2 Model description

2.1 PFLOTRAN

PFLOTRAN is a massively-parallel multi-physics simulator [*Hammond et al.*, 2014] developed and distributed under an open source GNU LGPL license and is freely available through Bitbucket (https://bitbucket.org/pflotran/pflotran-dev). It solves a system of generally nonlinear partial differential equations (PDEs) describing multiphase, multicomponent and multiscale reactive flow and transport in porous materials. The PDEs are spatially discretized using a finite volume technique, and the backward Euler scheme is used for implicit time discretization. It has been widely used for simulating subsurface multiphase flow and reactive biogeochemical

Geosci. Model Dev. Discuss., doi:10.5194/gmd-2017-35, 2017
Manuscript under review for journal Geosci. Model Dev.
Discussion started: 17 February 2017

Geoscientific Model Development Discussions

transport processes [*Chen et al.*, 2013; *Chen et al.*, 2012; *Hammond and Lichtner*, 2010; *Hammond et al.*, 2011; *Kumar et al.*, 2016; *Lichtner and Hammond*, 2012; *Liu et al.*, 2016; *Pau et al.*, 2014]

PFLOTRAN is written in object-oriented Fortran 2003/2008 and relies on the PETSc framework [*Balay et al.*, 2015] to provide the underlying parallel data structures and solvers for scalable high performance computing. PFLOTRAN uses domain decomposition and MPI libraries for parallelization. PFLOTRAN has been run on problems composed of over 3 billion degrees of freedom with up to 262,144 processors, but it is more commonly employed on problems with millions to tens of millions of degrees of freedom utilizing hundreds to thousands of processors. Although PFLOTRAN is designed for massively parallel computation, the same code base can be run on a single processor without recompiling, which may limit problem size based on available memory.

In this study, PFLOTRAN is used to simulate single phase variably saturated flow and solute transport in the subsurface. Single-phase variably saturated flow is based on the Richards equation with the form

$$\frac{\partial}{\partial t}(\varphi s \rho) + \nabla \cdot \rho \boldsymbol{q} = 0, \quad (1)$$

with water density ρ, porosity φ, and saturation s. The Darcy velocity, $\boldsymbol{q}$, is given by

$$\boldsymbol{q} = -\frac{k k_r}{\mu} \nabla(p - \rho g \boldsymbol{z}), \quad (2)$$

with water pressure p, viscosity μ, acceleration of gravity g, intrinsic permeability k, relative permeability k_r and elevation above a given datum z. Conservative solute transport in the liquid phase is based on the advection-dispersion equation

$$\frac{\partial}{\partial t}(\varphi s C) + \nabla \cdot (\boldsymbol{q} - \varphi s D \nabla) C = 0, \quad (3)$$

with solute concentration C and hydrodynamic dispersion coefficient D. PFLOTRAN employs backward Euler time discretization and finite volume spatial discretization. The discretized set of nonlinear equations for flow and transport are solved by the Newton-Raphson method.

Geosci. Model Dev. Discuss., doi:10.5194/gmd-2017-35, 2017
Manuscript under review for journal Geosci. Model Dev.
Discussion started: 17 February 2017

Geoscientific Model Development Discussions

2.2 The Community Land Model version 4.5

CLM4.5 [*Oleson et al.*, 2013] is the land component of the Community Earth System Model version 1 (CESM1) [*Hurrell et al.*, 2013], a fully coupled numerical simulator of the Earth system consisting of atmospheric, ocean, ice, land surface, carbon cycle, and other components (top panel of Figure 1). It has been applied successfully to explore interactions among water, energy, carbon, and biogeochemical cycling at local to global scales [*Leng et al.*, 2016b; *Xu et al.*, 2016], and proven to be highly scalable on leading HPC facilities such as the U.S. Department of Energy (USDOE)'s National Energy Research Scientific Computing Center (NERSC). The model includes parameterizations of terrestrial hydrological processes including interception, throughfall, canopy drip, snow accumulation and melt, water transfer between snow layers, infiltration, evaporation, surface runoff, sub-surface drainage, redistribution within the soil column, and groundwater discharge and recharge to simulate changes in canopy water, surface water, snow water, soil water, and soil ice, and water in the unconfined aquifer [*Oleson et al.*, 2013]. Precipitation is either intercepted by the canopy, falls directly to the snow/soil surface (throughfall), or drips off the vegetation (canopy drip). Water input at the land surface, the sum of liquid precipitation reaching the ground and melt water from snow, is partitioned into surface runoff, surface water storage, and infiltration into the soil. Two sets of runoff generation parameterizations, including formulations for saturation and infiltration excess runoff and baseflow, are implemented into the model: the TOPMODEL-based runoff generation formulations [*Beven and Kirkby*, 1979; *Niu et al.*, 2005; *Niu et al.*, 2007] and the Variable Infiltration Capacity (VIC)-based runoff generation formulations [*Lei et al.*, 2014; *Liang et al.*, 1994; *Wood et al.*, 1992]. Surface water storage and outflow in and from wetlands and small sub-grid scale water bodies are parameterized as functions of fine-spatial-scale elevation variations called microtopography. Soil water is predicted from a multi-layer model based on the 1-D Richards equation, with boundary conditions and source/sink terms specified as infiltration, surface and sub-surface runoff, gradient diffusion, gravity, canopy transpiration through root extraction, and interactions with groundwater. A groundwater component is added in the form of an unconfined aquifer lying below the soil column following *Niu et al.* [2007].

Geosci. Model Dev. Discuss., doi:10.5194/gmd-2017-35, 2017
Manuscript under review for journal Geosci. Model Dev.
Discussion started: 17 February 2017

2.3 Model coupling

A model interface layer was developed to couple PFLOTRAN and CLM4.5, including some key design features of the CESM coupler [*Craig et al.*, 2012] to support (i) different model domain decompositions and (ii) different grid resolutions. Both models support distributed memory parallelism via MPI, but perform domain decomposition across multiple processors differently. While CLM4.5 uses a round-robin decomposition approach, PFLOTRAN employs domain decomposition via PETSc. The model interface is developed to allow each model to support its native domain decomposition when run as a coupled model. The interface also allows the two models to run on different resolution grids and uses mapping files to regrid data for transfer between the two models. Analogous to the CESM coupler, the mapping files are generated as a pre-processing step in a format similar to the mapping files produced by the ESMF_RegridWeightGen (https://www.earthsystemcog.org/projects/regridweightgen). The model interface uses PETSc data structures to efficiently handle cross-processor communication and sparse matrix-vector products for mapping data from one grid to another. A schematic representation of the coupling between PFLOTRAN and CLM4.5 (within the CESM1 framework) is shown in top panel of Figure 1.

For the coupled PFLOTRAN_CLM v1.0 model, PFLOTRAN describes the subsurface flow and solute transport while CLM4.5 simulates the land surface processes. The carbon and nitrogen cycling can be solved in either PFLOTRAN or CLM4.5 but are not enabled in this study. For a given time step, CLM4.5 first computes infiltration, evaporation, and transpiration within the domain. The CLM4.5-simulated water sources and sinks are then used as prescribed conditions in the flow and transport simulation by PFLOTRAN. The soil moisture and soil hydraulic properties simulated by PFLOTRAN are then provided to CLM4.5 for simulating land water- and energy- budget terms in the next step. The bottom panel of Figure 1 shows a schematic representation of how stream-aquifer-land interactions are simulated in PFLOTRAN_CLM v1.0 when applied to the field scale, such as the 300 Area domain to be introduced in section 3.1. We note that in recent years, efforts have been made to implement carbon–nitrogen decomposition, nitrification, denitrification, and plant uptake from CLM4.5 in the form of a reaction network solved by PFLOTRAN to enable the coupling of biogeochemical processes between the two models [*Tang et al.*, 2016]. However, to our knowledge, this study represents the first description and application with a fully three-dimensional coupling between the hydrologic components of the two models enabled.

3 Site description and model configuration

3.1 The Hanford site and the 300 Area

The Hanford Reach is a stretch of the lower Columbia River extending approximately 55 km from the Priest Rapids hydroelectric dam to the outskirts of Richland, Washington, USA (Figure 2a) [*Tiffan et al.*, 2002]. The Columbia River above Priest Rapids Dam drains primarily mountainous regions in Canada, Idaho, Montana, and Washington, over which spatio-temporal distributions of precipitation and snowmelt modulate the timing and magnitude of river flows [*Elsner et al.*, 2010; *Hamlet and Lettenmaier*, 1999]. The Columbia River is highly regularted by dams for power generation and river stage and discharge along the Hanford Reach displays significant variation on multiple time scales. Strong seasonal variations occur with the greatest discharge (up to 12,000 m^3 s^{-1}) occurring from May through July due to snow melt, with less discharge (>1,700 m^3 s^{-1}) and lower flows occurring in the fall and winter [*Hamlet and Lettenmaier*, 1999; *Waichler et al.*, 2005]. Significant variation in discharge also occurs on a daily or hourly basis due to power generation, with fluctuations in river stage of up to 2 m within a 6-24 hr period being common [*Tiffan et al.*, 2002].

The Hanford site features an unconfined aquifer developed in Miocene-Pliocene fluvial and lacustrine sediments of the Ringold Formation, overlain by Pleistocene flood gravels of the Hanford formation [*Thorne et al.*, 2006] that is in hydrologic continuity with the Columbia River. The Hanford formation gravel and sand, deposited by glacial outburst floods at the end of the Pleistocene [*Bjornstad*, 2007], has a high average hydraulic conductivity at ~3,100 m d^{-1} [*Williams et al.*, 2008]. The fluvial deposits of the Ringold Formation have much lower hydraulic conductivity than the Hanford but are still relatively conductive at 36 m d^{-1} [*Williams et al.*, 2008]. Fine-grained lacustrine Ringold silt has a much lower estimated hydraulic conductivity of 1 m d^{-1}. The hydraulic conductivity of recent alluvium lining the river channel is low relative to the Hanford formation, which tends to dampen the response of water table elevation in wells near the river when changes occur in river stage [*Hammond et al.*, 2011;

Geosci. Model Dev. Discuss., doi:10.5194/gmd-2017-35, 2017
Manuscript under review for journal Geosci. Model Dev.
Discussion started: 17 February 2017

Geoscientific Model Development Discussions

Williams et al., 2008]. Overall, the Columbia River through the Hanford Reach is a prime example of a hyporheic corridor with an extensive floodplain aquifer. It is consequently an ideal alluvial system for evaluating the capability of the coupled model in simulating stream-aquifer-land interactions.

The region is situated in a cold desert climate with temperatures, precipitation, and winds that are greatly affected by the presence of mountain barriers. The Cascade Range to the west creates a strong rain shadow effect by forming a barrier to moist air moving from the Pacific Ocean, while the Rocky Mountains and ranges to the north protect it from the more severe cold polar air masses and winter storms moving south across Canada. Meteorological data are collected by the Hanford Meteorological Monitoring Network (http://www.hanford.gov/page.cfm/hms), which collects meteorological data representative of the general climatic conditions for the Hanford site.

A segment of the hyporheic corridor in the Hanford 300 Area (300A) was chosen to evaluate the model's capability in simulating river-aquifer-land interactions. Located at the downstream end of the Hanford Reach, the impact of dam operations on river stage is relatively damped, exhibiting a typical variation of ~0.5 m within a day and 2-3 m in a year. The study domain covers an area of 400 m × 400 m along the Columbia River shoreline (Figure 2(b)). Aquifer sediments in the 300 Area are coarse grained and highly permeable [*Chen et al., 2013*; *Hammond and Lichtner, 2010*]. Coupled with dynamic river stage variations, the resulting system is characterized by stage-driven intrusion and retreat of river water into the adjacent unconfined aquifer system. During high-stage spring runoff events, river water has been detected in monitoring wells nearly 400 m from the shoreline [*Williams et al.*, 2008]. During baseline, low-stage conditions (October-February), the Columbia River is a gaining stream, and the aquifer pore space is occupied by groundwater.

The study domain is instrumented with groundwater monitoring wells (Figure 2b) and a river gaging station that records water table elevations. A vegetation survey in 2015 was conducted to provide aerial coverages of grassland, shrubland, riparian trees in the domain (Figure 2b). A high-resolution topography and bathymetry dataset at 1-m resolution was assembled from multiple surveys by *Coleman et al.* [2010]. The data layers originated from Deep Water Bathymetric Boat surveys, terrestrial Light Detection and Ranging (LiDAR) surveys, and special

Geosci. Model Dev. Discuss., doi:10.5194/gmd-2017-35, 2017
Manuscript under review for journal Geosci. Model Dev.
Discussion started: 17 February 2017

Geoscientific Model Development Discussions
Open Access

hydrographic LiDAR surveys penetrating through water to collect both topographic and bathymetric elevation data.

3.2 Model configuration, numerical experiments, and analyses

To assess the effect of spatial resolution on simulated variables such as latent heat, sensible heat, water table depth, and river water in the domain, we configured PFLOTRAN_CLM v1.0 simulations at three horizontal spatial resolutions: 2-m, 10-m, and 20-m over the 400 m×400 m domain, respectively. For comparison purposes, we also configured a 2-m-resolution PFLOTRAN_CLM v1.0 vertical only simulation (i.e., $PFCLM_{v2m}$) in which lateral transfers of flow and solutes in the subsurface are disabled. Due to lack of observations of water and energy fluxes from the land surface, in this study we treat the 2-m-resolution PFLOTRAN_CLM v1.0 as the baseline and compare simulation results at other resolutions to it. New hydrologic regimes are projected to emerge over the Pacific Northwest in as early as the 2030s due to increases in winter precipitation and earlier snow melt in response to future warming [*Leng et al.*, 2016a]. Therefore, we expect that spring and early summer river discharge along the reach might increase in the future. To evaluate how land surface-subsurface coupling might be modulated hydro-climatic conditions, we designed additional numerical experiments by driving the model with elevated river stages by adding five meters to the observed river stage time series. The simulations and their configurations are summarized in Table 1.

The PFLOTRAN subsurface domain, also terrain-following and extending from soil surface (including riverbed) to 32 m below the surface, was discretized using a structured approach with rectangular grids. For the 2-m, 10-m, and 20-m resolution simulations, each mesh element was 2 m × 2 m, 10 m × 10 m, and 20 m×20 m, in the horizontal direction, and 0.5 m in the vertical direction, giving 2.56×10^6, 99.2×10^3, and 2.48×10^3 control volumes in total. The domain contained two materials with contrasting hydraulic conductivities: Hanford and Ringold (Figure 3). Note that only the soil moisture and soil hydraulic properties within the top 3.8 m are transferred from PFLOTRAN to CLM4.5 to allow simulations of infiltration, evaporation, and transpiration in the next time step, as the CLM4.5 subsurface domain is limited to 3.8 meters and cannot currently be easily modified. The hydrogeological properties of the Hanford and Ringold materials (Table 2) were taken from *Williams et al.* [2008]. The unsaturated hydraulic

Geosci. Model Dev. Discuss., doi:10.5194/gmd-2017-35, 2017
Manuscript under review for journal Geosci. Model Dev.
Discussion started: 17 February 2017

Geoscientific Model Development Discussions
Open Access

conductivity in PFLTORAN simulations was computed using the Van Genuchten water retention function [*van Genuchten*, 1980] and the Burdine permeability relationship [*Burdine*, 1953].

We applied time varying pressure boundary conditions to PFLOTRAN's subsurface domain at the northern, western, and southern boundaries. The transient boundary conditions were derived using kriging-based interpolations of hourly water table elevation measurements in wells inside and beyond the model domain, following the approach used by *Chen et al.* [2013]. Transient head boundary conditions were applied at the eastern boundary with water table elevations from the river gaging station and the gradient along the river estimated using water elevations simulated by a 1-D hydraulic model along the reach, the Modular Aquatic Simulation System in 1-Dimension (MASS1) [*Waichler et al.*, 2005], with a Nash–Sutcliffe coefficient [*Nash and Sutcliffe*, 1970] of 0.99 in the simulation period (figure not shown). The river stage simulated by MASS1 was also used to fill river stage measurement gaps caused by instrument failures. A conductance value of 10^{-12} m was applied to the eastern shoreline boundary to mimic the damping effect of low-permeability material on the river bed [*Hammond and Lichtner*, 2010]. A no-flow boundary condition was specified at the bottom of the domain to represent the basalt underlying the Ringold formation.

Vegetation types (Figure 2(b)) were converted to corresponding CLM4.5 plant functional types (PFTs) and bare soil (Figure 4). At each resolution, fractional area coverages of PFTs and bare soil are determined based on the base map and written into the surface dataset as CLM4.5 inputs (figures 4, S1, and S2). The CLM4.5 domain is terrain-following by treating the land surface as the top of the subsurface domain, which is hydrologically active to a depth of 3.8 m. The topography of the domain is retrieved from the 1-m topography and bathymetry dataset [*Coleman et al.*, 2010] based on the North American Vertical Datum of 1988 (NAD88) and resampled to each resolution (Figure S3).

The simulations were driven by hourly meteorological forcing from the Hanford meteorological stations and hourly river stage from the gaging station over the period of 2009-2015. Precipitation, wind speed, air temperature, and relative humidity were taken from the 300 Area meteorological station (longitude 119.726^{o}, latitude 46.578^{o}), located ~1.5 km from the modeling domain. Other meteorological variables, such as downward shortwave and longwave radiation, were obtained from the Hanford Meteorological station (longitude 119.599^{o}, latitude

46.563°) located in the center of the Hanford site. The first two years of simulations (i.e., 2009 and 2010) were discarded as the spin-up period, so that 2011-2015 is treated as the simulation period in the analyses.

Among the hydro-climatic forcing variables (e.g., river stage, surface air temperature, incoming shortwave radiation, and total precipitation), river stage displayed the greatest inter-annual variability (Figure 5). During the study period, high river stages occurred in early summer of 2011 and 2012 due to the melt of above-average winter snow packs in the upstream drainage basin, typical flow conditions occurred in 2013 and 2014, while 2015 was a year with low upstream snow accumulation. Meanwhile, the meteorological variables, especially temperature and shortwave radiation, do not show much inter-annual variability or trend, while precipitation in late spring (i.e., May) of 2012 is higher than that in the other years, coincident with the high river stage in 2012. In the "elevated" experiments (i.e., $PFCLM_{E2m}$, $PFCLM_{E10m}$, and $PFCLM_{E20m}$), the observed river stage (meters based on NAD88) was increased by five meters at each hourly time step to mimic a perturbed hydro-climatic condition in response to future warming.

To evaluate effects of river water and groundwater exchanges on land surface energy partitioning, we separated the study domain for the 2-m simulations with lateral water exchange (i.e., $PFCLM_{2m}$ and $PFCLM_{E2m}$) into two sub-domains based on 2-m topography (shown in Figure S3a): (a) the inland domain where the surface elevation is higher than 110 m; and (b) the riparian zone where the surface elevation is less than or equal to 110 m. In addition to the latent heat flux, the Bowen ratio, defined as the ratio between the sensible heat flux and latent heat flux, was calculated over the sub-domains for both observed and elevated conditions in the warm months (i.e., April to September) at a daily time step. The cold months were not included in this analysis to avoid numerical issues as a result of low energy inputs in combinations with water limitation in the winter, when LH could potentially become zero. The Bowen ratio is an indicator of the type of surface as summarized in literature [*Lewis*, 1995]: it is typically less than one over surfaces with abundant water supplies, ranges between 0.1-0.3, 0.4-0.8, 2.0-6.0 for tropical rainforests, temperate forests and grasslands, semi-arid landscapes, respectively, and becomes >10.0 over deserts.

Geosci. Model Dev. Discuss., doi:10.5194/gmd-2017-35, 2017
Manuscript under review for journal Geosci. Model Dev.
Discussion started: 17 February 2017

To better quantify the spatio-temporal dynamics of stream-aquifer interactions, a conservative tracer with a mole fraction of one was applied at the river boundary to track the flux of river water and its total mass in the subsurface domain. While a constant concentration was maintained at the river (i.e., eastern) boundary, the tracer was allowed to be transported out of the northern, western, and southern boundaries. Water infiltrating at the upper boundary based on CLM4.5 simulations was set to be tracer free, while a zero-flux tracer boundary condition was applied at the lower boundary. The initial flow condition was a hydrostatic pressure distribution based on the water table, as interpolated from the same set of wells that were used to create the transient lateral flow boundary conditions at the northern, western, and southern boundaries. The initial conservative tracer concentration was set to be zero for all mesh elements in the domain. The simulations were started on 1 January 2009 and the first two years were discarded as the spin-up period in the analysis. The mass of tracers in the domain and the fluxes of tracers across the boundary allow us to quantitatively understand how river water is retained and transported in the subsurface domain.

4 Results

4.1 Model validation

For the 3-D numerical experiments driven by the observed river stage time series (i.e., $PFCLM_{2m}$, $PFCLM_{10m}$, $PFCLM_{20m}$), PFLTORAN_CLM v1.0 simulated soil water pressure was converted to water table depth and compared against observed values at selected wells that were distributed throughout the domain and of variable distances from the river (Figure 6 and Table 3). The model performed very well in simulating the temporal dynamics of the water table at all resolutions. The root-mean-square errors were 0.028 m, 0.028 m, and 0.023 m at 2-m, 10-m, and 20-m resolutions, respectively. The corresponding Nash–Sutcliffe coefficients were 0.998, 0.998, and 0.999. It was surprising that the performance metrics at 20-m resolution outperform those at finer resolutions, but the differences were marginal given the close match between the model and observation. River stage was clearly the dominant driving factor for water table fluctuations at the inland wells. These results indicated that the coupled model was capable of simulating

Geosci. Model Dev. Discuss., doi:10.5194/gmd-2017-35, 2017
Manuscript under review for journal Geosci. Model Dev.
Discussion started: 17 February 2017

dynamic stream-aquifer interactions in the near shore groundwater aquifer that experiences pressure changes induced by river stage variations at sub-daily time scales.

4.2 Effect of stream-aquifer interactions on land surface energy partitioning

Next we evaluated the role of water table fluctuations on land surface variables, including latent heat (LH) and sensible heat (SH) fluxes. The site is characterized by an approximate 10 m vadose zone and surface fluxes and groundwater dynamics are typically decoupled [*Maxwell and Kollet*, 2008], especially over the inland portion of the domain covered by shallow-rooted PFTs and with higher surface elevations. However, river discharge and water table elevation displayed large seasonal and inter-annual variability in the study period. Therefore, we selected the month of June in each year to assess potential land surface-groundwater coupling because it is the month of peak river stage, while energy input is high and relatively constant across the years (Figure 7a).

In June 2011 and 2012, high river stages push the groundwater table to ~108 m (or ~6 m below the land surface). Groundwater at that elevation can affect land surface water and energy exchanges with the atmosphere. The shrubs, including the patch of Basin big sagebrush and the mixture of rabbitbrush and bunchgrass on the slope close to the river, are able to tap into the elevated water table with their deeper roots. In the inland portion of the domain, capillary supply was most evident in high-water years (i.e., 2011 and 2012), remains influential in normal years (i.e., 2013 and 2014), and is essentially disabled in low-water years (i.e., 2015). The lateral discharge of shallow groundwater to the river led to a band of negative difference in LH between $PFCLM_{2m}$ and $PFCLM_{v2m}$ at the river boundary when the stage was low due to a decrease in rooting zone soil moisture for evapotranspiration by the riparian trees (Figure 7b). This pattern was most evident in June 2015. Such a mechanism decreases in high-water and normal years because of more frequent inundation of the river bank and groundwater gradient reversal.

Driven by elevated river stages, land surface energy partitioning in $PFCLM_{E2m}$ (figures 8 and 9) was significantly shifted from that in $PFCLM_{2m}$ (Figure 7a) through two mechanisms: (1) expanding the periodically inundated fraction of the riparian zone (i.e., surface elevation ≤ 110 m); and (2) enhancing moisture availability in the vadose zone in the inland domain (i.e., surface elevation > 110 m) through capillary rise. Both mechanisms led to general increases in simulated vadose-zone moisture availability and therefore higher latent heat fluxes compared to the simulations driven by the observed condition. For the inland domain, Bowen ratios in the warm season clearly displayed a declining trend as the groundwater table level increased (i.e., shallower), consistent between the simulations (Figure 9a). 75% of the daily Bowen ratios for the inland domain stayed mostly > 5.0 when the water table levels are less than 108 m, suggesting decoupled surface-subsurface conditions in a typical semi-arid environment. When water table levels increased to be above 108 m, the coupling between the land surface energy budget and groundwater dynamics became stronger. As the elevation of the land surface is around 114-115 m, indicating that the water table fluctuated within the 6 m to 7 m range from the land surface, surface and subsurface processes were coupled, consistent with literature findings [*Leung et al.*, 2011; *Maxwell and Kollet*, 2008]. Consequently, 50-75% of the daily Bowen ratio values stayed well below 5.0 because of improved water availability for evapotranspiration, especially in the elevated simulation (i.e., $PFCLM_{E2m}$). Bowen ratios in the riparian zone remained within the range of [-1.0, 1.0], suggesting strong influences of the river and the role of deeper rooted plant types (e.g., riparian trees and shrubs) in modulating the energy partitioning (Figure 9) of riparian zones in the semi-arid to arid environments.

To confirm the above findings, the liquid saturation [*unitless*] and mass of river water [*mol*] in the domain from $PFCLM_{2m}$ and $PFCLM_{E2m}$ on 30 June each year are plotted along a transect perpendicular to the river (*y* = 200 m) in figures 10 and S4, and across a x-y plane at an elevation of 107 m in figures S5 and S6, respectively. Driven by the pressure introduced by elevated river stages, river water not only intruded further toward or even across the western boundary in high water years, but also led to shallower water table and increased liquid saturation in the vadose zone due to capillary rise across the domain. In fact, liquid saturation in the shallow vadose zone could increase from 0.1-0.2 in $PFCLM_{2m}$ to 0.3-0.4 in $PFCLM_{E2m}$ on these days because of river water intrusion. And the river-water tracer could show up in the near-surface vadose zone at a distance of ~400 m from the river (Figure S4). Interestingly, by comparing the spatial distributions of river-water tracer in the low-water year (i.e., 2015) between the "observed" and "elevated" scenarios, the presence of river water in the domain was much less in the elevated scenario in terms of its spatial coverage (figures 10 and S4). This pattern suggests that after a number of years of enhanced river water intrusion into the domain, the hydraulic gradient between groundwater and river-water could be reversed, so that groundwater discharging might be expected more frequently in low-water years in a prolonged elevated scenario.

The responses of LH and Bowen ratio (figures 8 and 9) indicated that a tight coupling among stream, aquifer, and land surface processes occurred in the elevated scenario, which could become realistic in one to two decades for the study site, or for other sites along the Hanford reach characterized by lower elevations under the current condition.

4.3 Effect of spatial resolution

To apply the model to large-scale simulations or over a long time period, it is important to assess how the model performs at coarser resolution, as the 2-m simulations are computationally expensive. Here, we use the 2-m simulations (i.e., $PFCLM_{2m}$ and $PFCLM_{E2m}$) simulations as benchmarks for this assessment. That is, $PFCLM_{2m}$ and $PFCLM_{E2m}$ simulated variables are treated as the “truth” for “observed” and “elevated” river stage scenarios, and outputs from other simulations are compared to them to verify their performance. In the previous section, we showed that simulated water table levels from the model were virtually identical to observations. In this section, we further quantify biases of other variables of interest from the high-fidelity 2-m simulations.

The domain-averaged daily surface energy fluxes from $PFCLM_{2m}$ show clear seasonal patterns, which are consistent in terms of their magnitudes and timing, reflecting mean climate conditions at the site (Figure S6). Driven by elevated river stages, latent heat from $PFCLM_{E2m}$ is consistently higher than that from $PFCLM_{2m}$. The mean latent heat and sensible heat fluxes simulated by $PFCLM_{2m}$ were 14.1 W m^{-2} and 38.7 W m^{-2} over this period, compared to by 18.50 W m^{-2} and 35.75 W m^{-2} in $PFCLM_{E2m}$. Figure 11 shows deviations of simulated LH and SH in the 20-m and 10-m simulations from the corresponding 2-m simulations. The deviations of both LH and SH were small across all the simulations driven by the observed river stage when surface and subsurface were decoupled. In the elevated simulations (i.e., $PFCLM_{E10m}$ and $PFCLM_{E20m}$) when surface and subsurface processes are more tightly coupled, errors in surface fluxes became significant in the coarse resolution simulations when compared to $PFCLM_{E2m}$. For example, the relative errors in LH were 2.41% and 1.35% for $PFCLM_{20m}$ and $PFCLM_{10m}$, respectively, as compared to $PFCLM_{2m}$, but grew as large as 33.84% and 33.19% for $PFCLM_{E20m}$ and

$PFCLM_{E10m}$, respectively, when compared to $PFCLM_{E2m}$. The 10-m simulations outperformed the 20-m simulations under both scenarios but the magnitudes of errors were comparable. On the other hand, notably the vertical only simulation ($PFCLM_{v2m}$) has a small error of 5.67% in LH compared to $PFCLM_{2m}$, indicating that lateral flow is less important when water table is deep.

To better understand how water in the river and the aquifer was connected, we also quantified the biases of subsurface state variables and fluxes including total water mass and tracer amount, as well as exchange rates of water and tracer at four boundaries of the subsurface domain using a similar approach (Figure S7 and Figure 12). Compared to the magnitude of total water mass in the domain (averaged 919.45 $\times10^6$ Kg and 1020.19 $\times10^6$ Kg in $PFCLM_{2m}$ and $PFCLM_{E2m}$), errors introduced by coarsening the resolution were very small under the observed river stage condition (0.04% for $PFCLM_{20m}$ and 0.03% for $PFCLM_{10m}$) and grew to 9.85% for $PFCLM_{E20m}$ and 9.87% for $PFCLM_{E10m}$ in terms of total water mass in the domain (Table 5). However, for total tracer in the domain (averaged 142.07$\times10^6$ mol and 172.46 $\times10^6$ mol in $PFCLM_{2m}$ and $PFCLM_{E2m}$) as a result of transport of river water in lateral and normal directions to the river, resolution clearly makes a difference under both observed condition and elevated scenarios (relative errors of 5.44% for $PFCLM_{10m}$, 10.40% for $PFCLM_{20m}$, and 22.0% for both $PFCLM_{E10m}$ and $PFCLM_{E20m}$). The magnitude of computed mass exchange rates at the four boundaries (Figure 12) indicates that a coarse resolution promotes larger river water fluxes and groundwater exchanges, especially during the period of spring river stage increase under the elevated scenario. This forcing contributes to a significant bias in total tracer amount by the end of the simulation. The exchange rates at the other three boundaries follow the same pattern but with smaller magnitudes, especially for the west boundary that requires a significant gradient high enough to push river water further inland.

The results of simulations at three different resolutions indicated that: (1) the partitioning of the land surface energy budget is mainly controlled by near-surface moisture. Spatial resolution did not seem to be a significant factor in the computation of surface energy fluxes when the water table was deep at the semi-arid site; (2) if the surface and subsurface are tighly coupled as in the elevated river stage simulations, resolution becomes an important factor to consider for credible simulations of the surface fluxes, as the land surface, subsurface, and riverine processes are expected to be more connected and coupled; (3) regardless of whether a tight coupling between the surface and subsurface occurs, if mass exchange rates and associated

Geosci. Model Dev. Discuss., doi:10.5194/gmd-2017-35, 2017
Manuscript under review for journal Geosci. Model Dev.
Discussion started: 17 February 2017

Geoscientific Model Development Discussions
Open Access
EGU

biogeochemical reactions in the aquifer are of interest, a higher resolution is desired close to the river shoreline to minimize terrain errors.

5 Conclusion and future work

A fully coupled three-dimensional surface and subsurface land model was developed and applied to a site along the Columbia River to simulate interactions among river water, groundwater, and land surface processes. The model features the coupling of the open-source and state-of-the-art models portable on HPCs, the multi-physics reactive transport model PFLOTRAN and the CLM4.5. Both models are under active development and testing by their respective communities, therefore the coupled model could be updated to newer versions of PFLOTRAN and/or CLM to facilitate transfer of knowledge in a seamless fashion. The integrated model represents a new addition to the integrated surface and subsurface suite of models.

By applying the coupled model to a field site along the Columbia River shoreline driven by highly dynamic river boundary conditions resulting from upstream dam operations, we demonstrated that the model can be used to advance mechanistic understanding of stream-aquifer-land interactions surrounding near-shore alluvial aquifers that experience pressure changes induced by river stage variations along managed river reaches, which are of global significance as a result of over 30,000 dams constructed worldwide during the past half century. The land surface, subsurface, and riverine processes along such managed river corridors are expected to be more strongly coupled under projected hydro-climatic regimes as a result of increases in winter precipitation and early snowmelt. The dataset presented in this study can serve as a good benchmarking case for testing other integrated models for their applications to such systems. More data needs to be collected to facilitate the application and validation of the model to a larger domain for understanding the contribution of near-shore hydrologic exchange to water retention, biogeochemical cycling, and ecosystem functions along the river corridors.

By benchmarking the coarser resolution simulations at 20 m and 10 m against the 2-m simulations, we find that resolution is not a significant factor for surface flux simulations when the water table is deep. However, resolution becomes important when the surface and subsurface processes are tightly coupled, and for accurately estimating the rate of mass exchange at the

Geosci. Model Dev. Discuss., doi:10.5194/gmd-2017-35, 2017
Manuscript under review for journal Geosci. Model Dev.
Discussion started: 17 February 2017

riverine boundaries, which can affect the calculation of biogeochemical processes involved in carbon and nitrogen cycles.

Our numerical experiments suggested that riverine, land surface, and subsurface processes could become more tightly coupled through two mechanisms in the near-shore environments: (1) expanding the periodically inundated fraction of the riparian zone and (2) enhancing moisture availability in the vadose zone in the inland domain through capillary rise. Both mechanisms can lead to increases in vadose-zone moisture availability and higher evapotranspiration rates. The latter is critical for understanding ecosystem functioning, biogeochemical cycling, and land-atmosphere interactions along river corridors in arid and semi-arid regions that are expected to experience new hydro-climatic regimes in a changing climate. However, these systems have been poorly accounted for in current-generation Earth system models and therefore require more attention in future studies.

Code availability

PFLOTRAN is open-source software. It is distributed under the terms of the GNU Lesser General Public License as published by the Free Software Foundation either version 2.1 of the License, or any later version. It is available at https://bitbucket.org/pflotran. CLM4.5 is also open-source software released as part of the Community Earth System Model (CESM) version 1.2 (http://www.cesm.ucar.edu/models/cesm1.2). PFLOTRAN_CLM v1.0 is under development and will be made available upon request.

Geoscientific Model Development Discussions Open Access EGU

Acknowledgement

This research was supported by the U.S. Department of Energy (DOE), Office of Biological and Environmental Research (BER), as part of BER's Subsurface Biogeochemical Research Program (SBR). This contribution originates from the SBR Scientific Focus Area (SFA) at the Pacific Northwest National Laboratory (PNNL).

References

Balay, S., J. Brown, K. Buschelman, V. Eijkhout, W. D. Gropp, D. Kaushik, M. G. Knepley, L. C. McInnes, B. F. Smith, and H. Zhang (2015), PETSc Users Manual, Tech. Rep. ANL-95/11—Revision 3.5*Rep.*, Argonne, Ill.

Beven, K. J., and M. J. Kirkby (1979), A physically based, variable contributing area model of basin hydrology / Un modèle à base physique de zone d'appel variable de l'hydrologie du bassin versant, *Hydrological Sciences Bulletin*, *24*(1), 43-69, doi:10.1080/02626667909491834.

Bjornstad, B. N. (2007), *On the Trail of the Ice Age Floods: A Geological Field Guide to the Mid-Columbian Basin*, KeoKee, Sandpoint, ID.

Burdine, N. T. (1953), Relative Permeability Calculations From Pore Size Distribution Data, doi:10.2118/225-G.

Chen, X., G. E. Hammond, C. J. Murray, M. L. Rockhold, V. R. Vermeul, and J. M. Zachara (2013), Application of ensemble-based data assimilation techniques for aquifer characterization using tracer data at Hanford 300 area, *Water Resources Research*, *49*(10), 7064-7076, doi:10.1002/2012WR013285.

Chen, X., H. Murakami, M. S. Hahn, G. E. Hammond, M. L. Rockhold, J. M. Zachara, and Y. Rubin (2012), Three-dimensional Bayesian geostatistical aquifer characterization at the Hanford 300 Area using tracer test data, *Water Resources Research*, *48*(6), n/a-n/a, doi:10.1029/2011WR010675.

Clark, M. P., et al. (2015), Improving the representation of hydrologic processes in Earth System Models, *Water Resources Research*, *51*(8), 5929-5956, doi:10.1002/2015WR017096.

Coleman, A., K. Larson, D. Ward, and J. Lettrick (2010), Development of a High-Resolution Bathymetry Dataset for the Columbia River through the Hanford Reach*Rep. PNNL-19878*, Pacific Northwest National Laboratory, Richland, WA.

Condon, L. E., R. M. Maxwell, and S. Gangopadhyay (2013), The impact of subsurface conceptualization on land energy fluxes, *Advances in Water Resources*, *60*(0), 188-203, doi:http://dx.doi.org/10.1016/j.advwatres.2013.08.001.

Craig, A. P., M. Vertenstein, and R. Jacob (2012), A new flexible coupler for earth system modeling developed for CCSM4 and CESM1, *International Journal of High Performance Computing Applications*, *26*(1), 31-42, doi:10.1177/1094342011428141.

Elsner, M. M., L. Cuo, N. Voisin, J. S. Deems, A. F. Hamlet, J. A. Vano, K. E. B. Mickelson, S. Y. Lee, and D. P. Lettenmaier (2010), Implications of 21st century climate change for the hydrology of Washington State, *Climatic Change*, *102*(1-2), 225-260, doi:DOI 10.1007/s10584-010-9855-0.

Fan, Y., H. Li, and G. Miguez-Macho (2013), Global Patterns of Groundwater Table Depth, *Science*, *339*(6122), 940-943.

Fan, Y., and G. Miguez-Macho (2011), A simple hydrologic framework for simulating wetlands in climate and earth system models, *Climate Dynamics*, *37*(1), 253-278, doi:10.1007/s00382-010-0829-8.

Fischer, H., F. Kloep, S. Wilzcek, and M. T. Pusch (2005), A river's liver - microbial processes within the hyporheic zone of a large lowland river, *Biogeochemistry*, *76*(2), 349-371.

Gaillardet, J., P. Regnier, R. Lauerwald, and P. Ciais (2014), Geochemistry of the Earth's surface GES-10 Paris France, 18-23 August, 2014.Carbon Leakage through the Terrestrial-aquatic Interface: Implications for the Anthropogenic CO2 Budget, *Procedia Earth and Planetary Science*, *10*, 319-324, doi:http://dx.doi.org/10.1016/j.proeps.2014.08.025.

Hamlet, A. F., and D. P. Lettenmaier (1999), Effects of climate change on hydrology and water resources in the Columbia River basin, *Journal of the American Water Resources Association*, *35*(6), 1597-1623.

Hammond, G. E., and P. C. Lichtner (2010), Field-scale model for the natural attenuation of uranium at the Hanford 300 Area using high-performance computing, *Water Resources Research*, *46*(9), n/a-n/a, doi:10.1029/2009WR008819.

Hammond, G. E., P. C. Lichtner, and R. T. Mills (2014), Evaluating the performance of parallel subsurface simulators: An illustrative example with PFLOTRAN, *Water Resources Research*, *50*(1), 208-228, doi:10.1002/2012WR013483.

Hammond, G. E., P. C. Lichtner, and M. L. Rockhold (2011), Stochastic simulation of uranium migration at the Hanford 300 Area, *Journal of Contaminant Hydrology*, *120-21*, 115-128, doi:DOI 10.1016/j.jconhyd.2010.04.005.

Harvey, J., and M. Gooseff (2015), River corridor science: Hydrologic exchange and ecological consequences from bedforms to basins, *Water Resources Research*, *51*(9), 6893-6922, doi:10.1002/2015WR017617.

Hou, Z., M. Huang, L. R. Leung, G. Lin, and D. M. Ricciuto (2012), Sensitivity of surface flux simulations to hydrologic parameters based on an uncertainty quantification framework applied to the Community Land Model, *Journal of Geophysical Research: Atmospheres (1984–2012)*, *117*(D15).

Hurrell, J. W., et al. (2013), The Community Earth System Model: A Framework for Collaborative Research, *Bulletin of the American Meteorological Society*, *94*(9), 1339-1360, doi:10.1175/bams-d-12-00121.1.

Ji, X., C. Shen, and W. J. Riley (2015), Temporal evolution of soil moisture statistical fractal and controls by soil texture and regional groundwater flow, *Advances in Water Resources*, *86, Part A*, 155-169, doi:http://dx.doi.org/10.1016/j.advwatres.2015.09.027.

Kollet, S. J., and R. M. Maxwell (2008), Capturing the influence of groundwater dynamics on land surface processes using an integrated, distributed watershed model, *Water Resources Research*, *44*(2), n/a-n/a, doi:10.1029/2007WR006004.

Kumar, J., N. Collier, G. Bisht, R. T. Mills, P. E. Thornton, C. M. Iversen, and V. Romanovsky (2016), Modeling the spatiotemporal variability in subsurface thermal regimes across a low-relief polygonal tundra landscape, *The Cryosphere*, *10*(5), 2241-2274, doi:10.5194/tc-10-2241-2016.

Lei, H., M. Huang, L. R. Leung, D. Yang, X. Shi, J. Mao, D. J. Hayes, C. R. Schwalm, Y. Wei, and S. Liu (2014), Sensitivity of global terrestrial gross primary production to hydrologic states simulated by the Community Land Model using two runoff parameterizations, *Journal of Advances in Modeling Earth Systems*, *6*(3), 658-679.

Geosci. Model Dev. Discuss., doi:10.5194/gmd-2017-35, 2017
Manuscript under review for journal Geosci. Model Dev.
Discussion started: 17 February 2017

Geoscientific Model Development Discussions
Open Access
EGU

Leng, G., M. Huang, N. Voisin, X. Zhang, G. R. Asrar, and L. R. Leung (2016a), Emergence of new hydrologic regimes of surface water resources in the conterminous United States under future warming, *Environmental Research Letters*, *11*(11), 114003.

Leng, G., X. Zhang, M. Huang, Q. Yang, R. Rafique, G. R. Asrar, and L. R. Leung (2016b), Simulating county-level crop yields in the conterminous United States using the community land model: The effects of optimizing irrigation and fertilization, *Journal of Advances in Modeling Earth Systems*, n/a-n/a, doi:10.1002/2016MS000645.

Leung, L. R., M. Huang, Y. Qian, and X. Liang (2011), Climate–soil–vegetation control on groundwater table dynamics and its feedbacks in a climate model, *Climate Dynamics*, *36*(1), 57-81.

Lewis, J. M. (1995), The Story behind the Bowen Ratio, *Bulletin of the American Meteorological Society*, *76*(12), 2433-2443, doi:10.1175/1520-0477(1995)076<2433:tsbtbr>2.0.co;2.

Liang, X., D. P. Lettenmaier, E. F. Wood, and S. J. Burges (1994), A simple hydrologically based model of land surface water and energy fluxes for general circulation models, *Journal of Geophysical Research: Atmospheres*, *99*(D7), 14415-14428, doi:10.1029/94JD00483.

Lichtner, P. C., and G. E. Hammond (2012), Using High Performance Computing to Understand Roles of Labile and Nonlabile Uranium(VI) on Hanford 300 Area Plume Longevity, *Vadose Zone Journal*, *11*(2), doi:10.2136/vzj2011.0097.

Lichtner, P. C., G. E. Hammond, C. Lu, S. Karra, G. Bisht, B. Andre, R. T. Mills, and K. Jitu (2015), PFLOTRAN User Manual: a Massively Parallel Reactive Flow and Transport Model for Describing Surface and Subsurface Processes*Rep.*

Liu, Y., G. Bisht, Z. M. Subin, W. J. Riley, and G. S. H. Pau (2016), A Hybrid Reduced-Order Model of Fine-Resolution Hydrologic Simulations at a Polygonal Tundra Site, *Vadose Zone Journal*, *15*(2).

Maxwell, R. M., and L. E. Condon (2016), Connections between groundwater flow and transpiration partitioning, *Science*, *353*(6297), 377-380, doi:10.1126/science.aaf7891.

Maxwell, R. M., L. E. Condon, and S. J. Kollet (2015), A high-resolution simulation of groundwater and surface water over most of the continental US with the integrated hydrologic model ParFlow v3, *Geosci. Model Dev.*, *8*(3), 923-937, doi:10.5194/gmd-8-923-2015.

Maxwell, R. M., and S. J. Kollet (2008), Interdependence of groundwater dynamics and land-energy feedbacks under climate change, *Nature Geosci*, *1*(10), 665-669.

Maxwell, R. M., and N. L. Miller (2005), Development of a Coupled Land Surface and Groundwater Model, *Journal of Hydrometeorology*, *6*(3), 233-247, doi:10.1175/JHM422.1.

Maxwell, R. M., et al. (2014), Surface-subsurface model intercomparison: A first set of benchmark results to diagnose integrated hydrology and feedbacks, *Water Resources Research*, *50*(2), 1531-1549, doi:10.1002/2013WR013725.

McNamara, J. P., D. Chandler, M. Seyfried, and S. Achet (2005), Soil moisture states, lateral flow, and streamflow generation in a semi-arid, snowmelt-driven catchment, *Hydrological Processes*, *19*(20), 4023-4038, doi:10.1002/hyp.5869.

Geosci. Model Dev. Discuss., doi:10.5194/gmd-2017-35, 2017
Manuscript under review for journal Geosci. Model Dev.
Discussion started: 17 February 2017

Miguez-Macho, G., and Y. Fan (2012), The role of groundwater in the Amazon water cycle: 1. Influence on seasonal streamflow, flooding and wetlands, *Journal of Geophysical Research: Atmospheres*, *117*(D15), n/a-n/a, doi:10.1029/2012JD017539.

Nash, J. E., and J. V. Sutcliffe (1970), River flow forecasting through conceptual models part I — A discussion of principles, *Journal of Hydrology*, *10*(3), 282-290, doi:http://dx.doi.org/10.1016/0022-1694(70)90255-6.

Nir, Y. K., L. Haibin, and F. Ying (2014), Groundwater flow across spatial scales: importance for climate modeling, *Environmental Research Letters*, *9*(3), 034003.

Niu, G.-Y., C. Paniconi, P. A. Troch, R. L. Scott, M. Durcik, X. Zeng, T. Huxman, and D. C. Goodrich (2014), An integrated modelling framework of catchment-scale ecohydrological processes: 1. Model description and tests over an energy-limited watershed, *Ecohydrology*, *7*(2), 427-439, doi:10.1002/eco.1362.

Niu, G.-Y., Z.-L. Yang, R. E. Dickinson, and L. E. Gulden (2005), A simple TOPMODEL-based runoff parameterization (SIMTOP) for use in global climate models, *Journal of Geophysical Research: Atmospheres*, *110*(D21), n/a-n/a, doi:10.1029/2005JD006111.

Niu, G.-Y., Z.-L. Yang, R. E. Dickinson, L. E. Gulden, and H. Su (2007), Development of a simple groundwater model for use in climate models and evaluation with Gravity Recovery and Climate Experiment data, *Journal of Geophysical Research: Atmospheres*, *112*(D7), n/a-n/a, doi:10.1029/2006JD007522.

Oleson, K. W., et al. (2013), Technical Description of version 4.5 of the Community Land Model (CLM)*Rep. Ncar Technical Note NCAR/TN-503+STR*, National Center for Atmospheric Research, Boulder, CO.

Pau, G. S. H., G. Bisht, and W. J. Riley (2014), A reduced-order modeling approach to represent subgrid-scale hydrological dynamics for land-surface simulations: application in a polygonal tundra landscape, *Geosci. Model Dev.*, *7*(5), 2091-2105, doi:10.5194/gmd-7-2091-2014.

Pau, G. S. H., C. Shen, W. J. Riley, and Y. Liu (2016), Accurate and efficient prediction of fine-resolution hydrologic and carbon dynamic simulations from coarse-resolution models, *Water Resources Research*, *52*(2), 791-812, doi:10.1002/2015WR017782.

Rahman, M., M. Sulis, and S. J. Kollet (2015), The subsurface-land surface-atmosphere connection under convective conditions, *Advances in Water Resources*, *83*, 240-249, doi:10.1016/j.advwatres.2015.06.003.

Rihani, J. F., F. K. Chow, and R. M. Maxwell (2015), Isolating effects of terrain and soil moisture heterogeneity on the atmospheric boundary layer: Idealized simulations to diagnose land-atmosphere feedbacks, *Journal of Advances in Modeling Earth Systems*, *7*(2), 915-937, doi:10.1002/2014MS000371.

Riley, W. J., and C. Shen (2014), Characterizing coarse-resolution watershed soil moisture heterogeneity using fine-scale simulations, *Hydrol. Earth Syst. Sci.*, *18*(7), 2463-2483, doi:10.5194/hess-18-2463-2014.

Schaller, M. F., and Y. Fan (2009), River basins as groundwater exporters and importers: Implications for water cycle and climate modeling, *Journal of Geophysical Research: Atmospheres*, *114*(D4), n/a-n/a, doi:10.1029/2008JD010636.

Shen, C., J. Niu, and M. S. Phanikumar (2013), Evaluating controls on coupled hydrologic and vegetation dynamics in a humid continental climate watershed using a subsurface-land surface processes model, *Water Resources Research*, *49*(5), 2552-2572, doi:10.1002/wrcr.20189.

Shen, C., W. J. Riley, K. M. Smithgall, J. M. Melack, and K. Fang (2016), The fan of influence of streams and channel feedbacks to simulated water and carbon fluxes, *Water Resources Research*, doi:10.1002/2015WR018086.

Shi, Y., K. J. Davis, C. J. Duffy, and X. Yu (2013), Development of a Coupled Land Surface Hydrologic Model and Evaluation at a Critical Zone Observatory, *Journal of Hydrometeorology*, *14*(5), 1401-1420, doi:10.1175/JHM-D-12-0145.1.

Tang, G., et al. (2016), Addressing numerical challenges in introducing a reactive transport code into a land surface model: a biogeochemical modeling proof-of-concept with CLM–PFLOTRAN 1.0, *Geosci. Model Dev.*, *9*(3), 927-946, doi:10.5194/gmd-9-927-2016.

Taylor, R. G., et al. (2013), Ground water and climate change, *Nature Clim. Change*, *3*(4), 322-329.

Thorne, P. D., M. P. Bergeron, M. D. Williams, and V. L. Freedman (2006), Groundwater Data Package for Hanford Assessments*Rep. PNNL-14753*, Pacific Northwest National Laboratory, Richland, WA.

Tiffan, K. F., R. D. Garland, and D. W. Rondorf (2002), Quantifying flow-dependent changes in subyearling fall chinook salmon rearing habitat using two-dimensional spatially explicit modeling, *North American Journal of Fisheries Management*, *22*(3), 713-726, doi:Doi 10.1577/1548-8675(2002)022<0713:Qfdcis>2.0.Co;2.

van Genuchten, M. T. (1980), A Closed-form Equation for Predicting the Hydraulic Conductivity of Unsaturated Soils1, *Soil Science Society of America Journal*, *44*(5), 892-898, doi:10.2136/sssaj1980.03615995004400050002x.

Waichler, S. R., W. A. Perkins, and M. C. Richmond (2005), Hydrodynamic Simulation of the Columbia River, Hanford Reach, 1940-2004*Rep. PNNL-15226*, Pacific Northwest National Laboratory, Richland, WA.

Williams, M. D., M. L. Rockhold, P. D. Thorne, and Y. Chen (2008), Three-Dimensional Groundwater Models of the 300 Area at the Hanford Site, Washington State*Rep. PNNL-17708*, Pacific Northwest National Laboratory, Richland, WA.

Wood, E. F., D. P. Lettenmaier, and V. G. Zartarian (1992), A land-surface hydrology parameterization with subgrid variability for general circulation models, *Journal of Geophysical Research: Atmospheres*, *97*(D3), 2717-2728, doi:10.1029/91JD01786.

Xu, X., et al. (2016), A multi-scale comparison of modeled and observed seasonal methane emissions in northern wetlands, *Biogeosciences*, *13*(17), 5043-5056, doi:10.5194/bg-13-5043-2016.

Zhang, B., J. L. Tang, C. Gao, and H. Zepp (2011), Subsurface lateral flow from hillslope and its contribution to nitrate loading in streams through an agricultural catchment during subtropical rainstorm events, *Hydrol. Earth Syst. Sci.*, *15*(10), 3153-3170, doi:10.5194/hess-15-3153-2011.

Geosci. Model Dev. Discuss., doi:10.5194/gmd-2017-35, 2017
Manuscript under review for journal Geosci. Model Dev.
Discussion started: 17 February 2017

Zhou, T., B. Nijssen, H. L. Gao, and D. P. Lettenmaier (2016), The Contribution of Reservoirs to Global Land Surface Water Storage Variations, *Journal of Hydrometeorology*, *17*(1), 309-325, doi:10.1175/jhm-d-15-0002.1.

Geosci. Model Dev. Discuss., doi:10.5194/gmd-2017-35, 2017
Manuscript under review for journal Geosci. Model Dev.
Discussion started: 17 February 2017

Tables and Figures

Table 1. Summary of numerical experiments

Experiments	Horizontal Resolution	Lateral flow	River Stage (m)
PFCLMv$_{2m}$	2m	No	Observed
PFCLM$_{2m}$	2m	Yes	Observed
PFCLM$_{10m}$	10m	Yes	Observed
PFCLM$_{20m}$	20m	Yes	Observed
PFCLM$_{E2m}$	2m	Yes	Observed +5
PFCLM$_{E10m}$	10m	Yes	Observed +5
PFCLM$_{E20m}$	20m	Yes	Observed +5

Geosci. Model Dev. Discuss., doi:10.5194/gmd-2017-35, 2017
Manuscript under review for journal Geosci. Model Dev.
Discussion started: 17 February 2017

Geoscientific Model Development Discussions Open Access EGU

Table 2. Hydrogeological material properties of Hanford and Ringold materials.

Material	Porosity	Permeability (m^2)	Van Genuchten/Burdine Parameters		
			Res. Sat.	m	alpha
Hanford	0.20	7.387×10^{-9}	0.16	0.34	7.27×10^{-4}
Ringold	0.40	1.055×10^{-12}	0.13	0.75	1.43×10^{-4}

Geosci. Model Dev. Discuss., doi:10.5194/gmd-2017-35, 2017
Manuscript under review for journal Geosci. Model Dev.
Discussion started: 17 February 2017

Geoscientific Model Development Discussions
Open Access
EGU

Table 3. The comparison between simulated and observed water table levels

Well number	**PFCLM$_{2m}$**		**PFCLM$_{10m}$**		**PFCLM$_{20m}$**	
	RMSE (m)	N-S	RMSE (m)	N-S	RMSE (m)	N-S
399-3-29	0.022	0.999	0.022	0.999	0.021	0.999
399-3-34	0.011	1.000	0.011	1.000	0.006	1.000
399-2-01	0.039	0.997	0.038	0.997	0.029	0.998
399-1-60	0.016	1.000	0.016	0.999	0.013	1.000
399-2-33	0.028	0.998	0.028	0.998	0.022	0.999
399-1-21A	0.023	0.999	0.023	0.999	0.020	0.999
399-2-03	0.037	0.997	0.037	0.997	0.029	0.998
399-2-02	0.045	0.995	0.045	0.995	0.042	0.996
mean	0.028	0.998	0.028	0.998	0.023	0.999

Geosci. Model Dev. Discuss., doi:10.5194/gmd-2017-35, 2017
Manuscript under review for journal Geosci. Model Dev.
Discussion started: 17 February 2017

Geoscientific Model Development Discussions
Open Access
EGU

Table 4. The relative error in surface energy fluxes simulated by $PFCLM_{10m}$ and $PFCLM_{20m}$ benchmarked against $PFCLM_{2m}$ and by $PFCLM_{E10m}$ and $PFCLM_{E20m}$ benchmarked against $PFCLM_{E2m}$

Simulation	***Latent heat flux (%)***	***Sensible heat flux (%)***
$PFCLM_{v2m}$	5.67	1.63
$PFCLM_{10m}$	1.35	0.78
$PFCLM_{20m}$	2.41	1.42
$PFCLM_{E10m}$	33.19	13.71
$PFCLM_{E20m}$	33.84	14.18

Table 5. The relative error in total water mass and tracer amount in the subsurface simulated by $PFCLM_{10m}$ and $PFCLM_{20m}$ benchmarked against $PFCLM_{2m}$ and by $PFCLM_{E10m}$ and $PFCLM_{E20m}$ benchmarked against $PFCLM_{E2m}$

Simulation	Total water mass (%)	Total tracer (%)
$PFCLM_{10m}$	0.03	5.44
$PFCLM_{20m}$	0.04	10.40
$PFCLM_{E10m}$	9.87	22.00
$PFCLM_{E20m}$	9.85	22.00

Geosci. Model Dev. Discuss., doi:10.5194/gmd-2017-35, 2017
Manuscript under review for journal Geosci. Model Dev.
Discussion started: 17 February 2017

Geoscientific Model Development
Open Access
Discussions

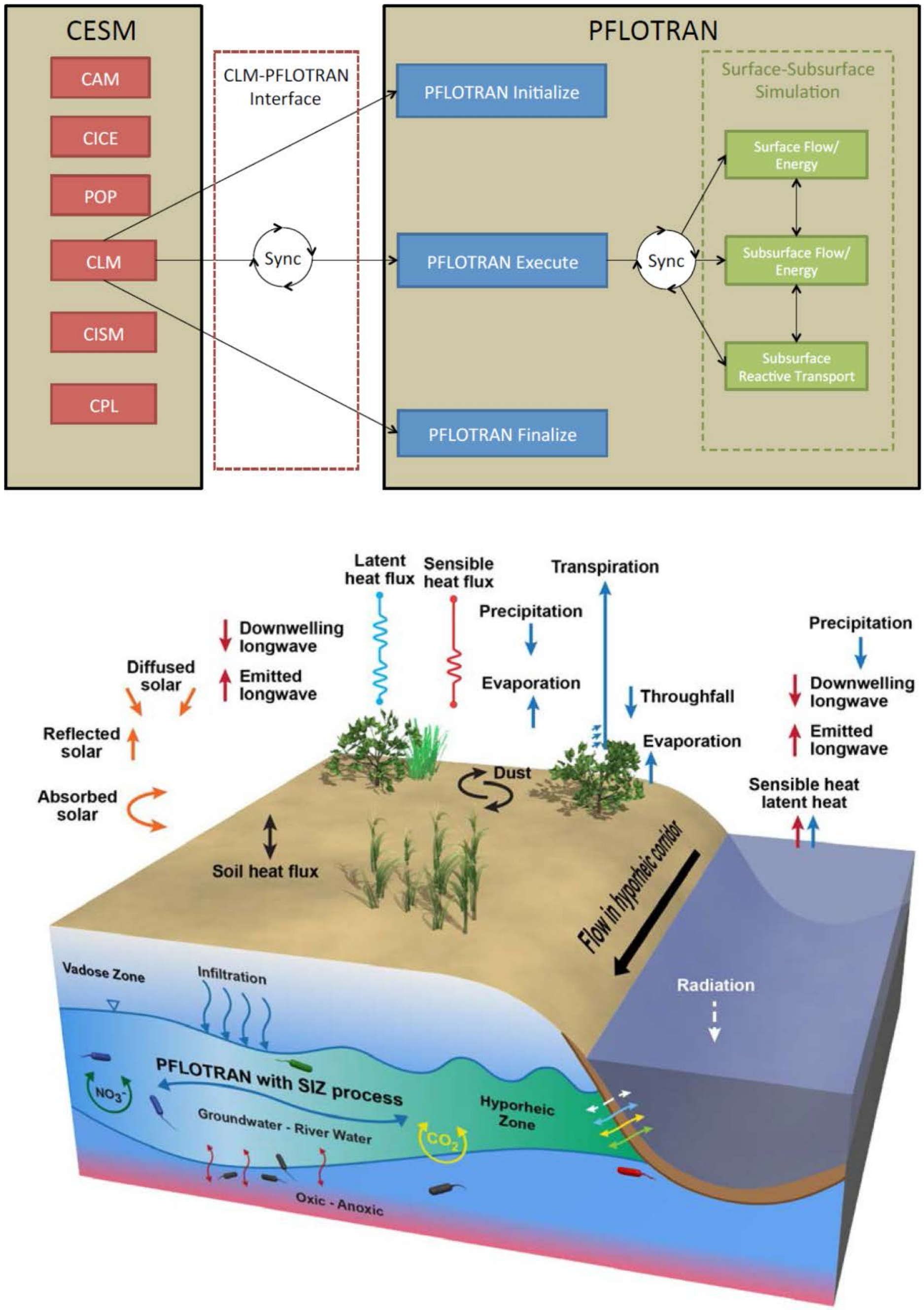

Figure 1. Schematic representations of (Top) the model coupling interface of PFLOTRAN_CLM v1.0, and (Bottom) hydrologic processes simulated in PFLOTRAN_CLM v1.0.

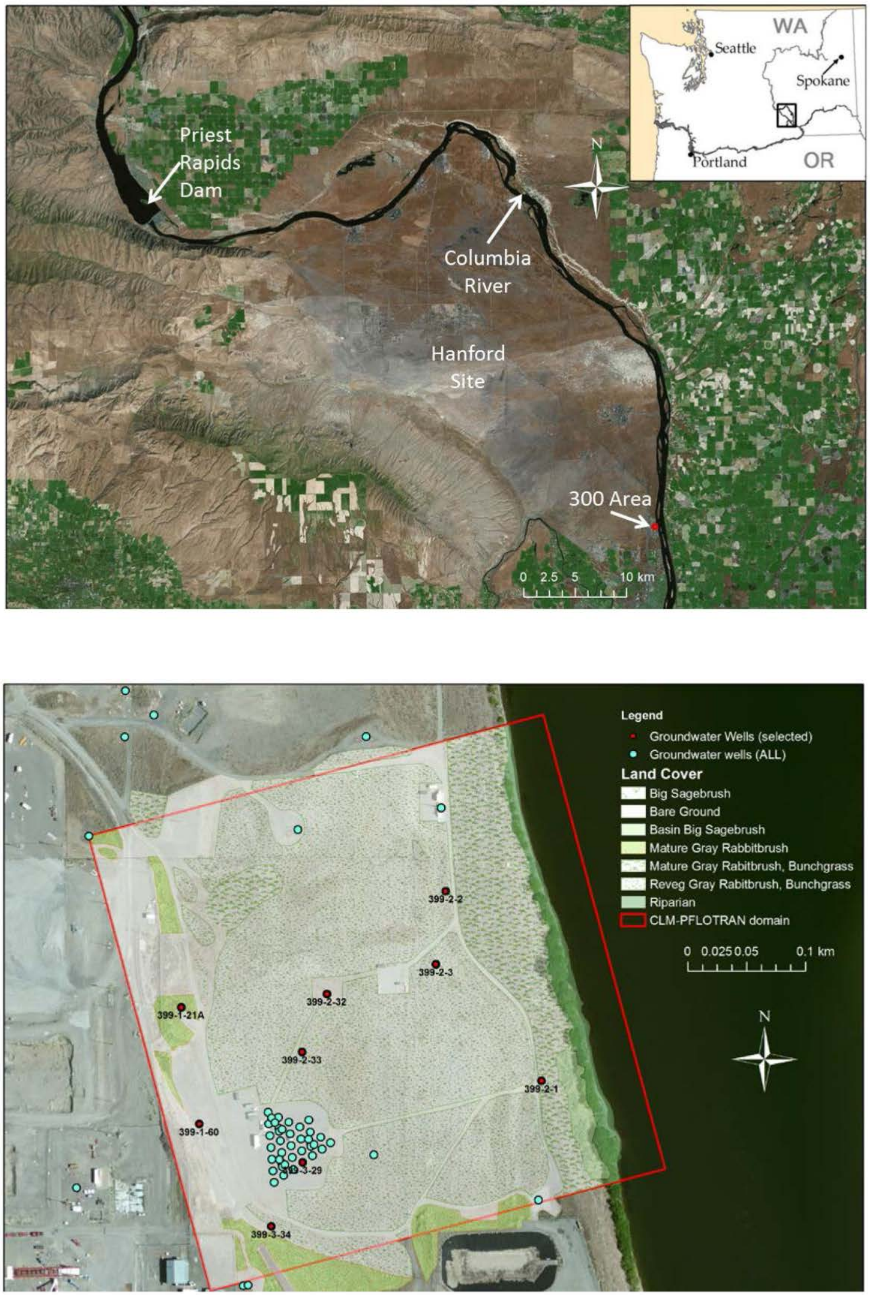

Figure 2. (Top) The Hanford Reach of the Columbia River and the Hanford Site location in south-central Washington State, USA; (Bottom) the 400 m × 400 m modeling domain located in the Hanford 300 Area.

Geoscientific Model Development
Discussions
Open Access

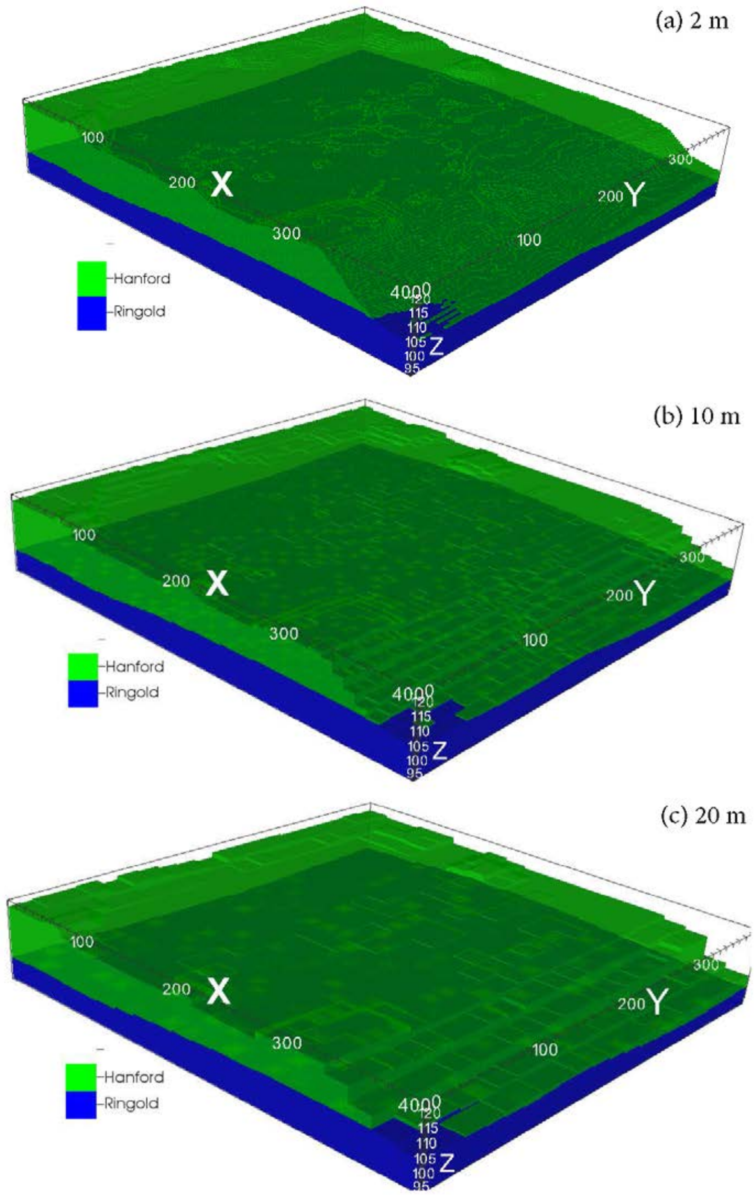

Figure 3. PFLOTRAN meshes and associated material IDs at (a) 2-m; (b) 10-m; and (c) 20-m resolutions

Geosci. Model Dev. Discuss., doi:10.5194/gmd-2017-35, 2017
Manuscript under review for journal Geosci. Model Dev.
Discussion started: 17 February 2017

Geoscientific Model Development
Discussions

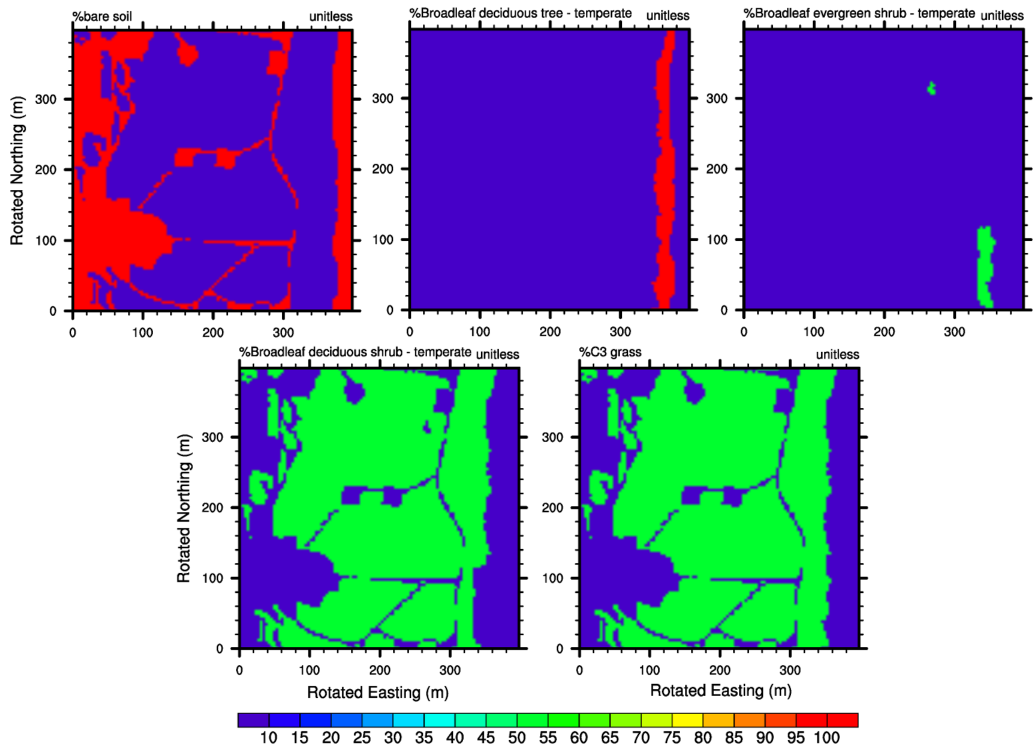

Figure 4. Plant function types at 2-m resolution as inputs for CLM4.5

Geosci. Model Dev. Discuss., doi:10.5194/gmd-2017-35, 2017
Manuscript under review for journal Geosci. Model Dev.
Discussion started: 17 February 2017

Geoscientific Model Development Discussions
Open Access

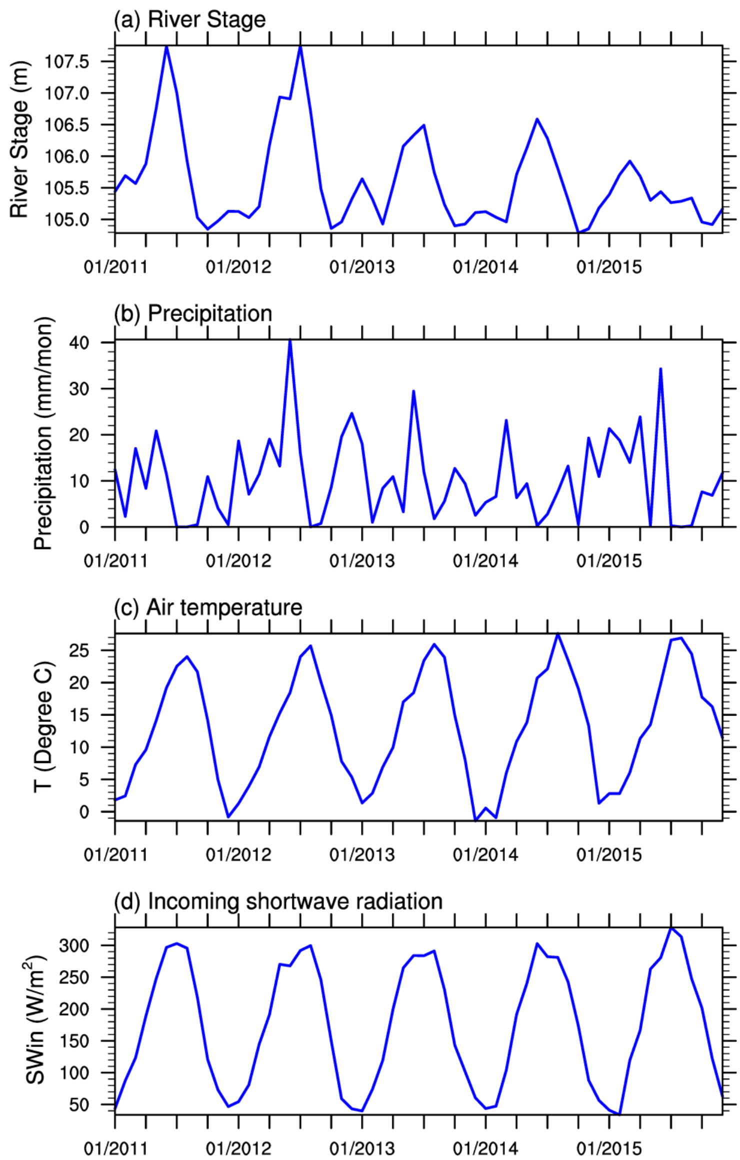

Figure 5. Hydro-meteorological drivers in the study period: (a) monthly mean river Stage; (b) monthly total precipitation; (c) monthly mean surface air temperature; (d) and monthly mean incoming shortwave radiation.

Geosci. Model Dev. Discuss., doi:10.5194/gmd-2017-35, 2017
Manuscript under review for journal Geosci. Model Dev.
Discussion started: 17 February 2017

Geoscientific Model Development Discussions
Open Access

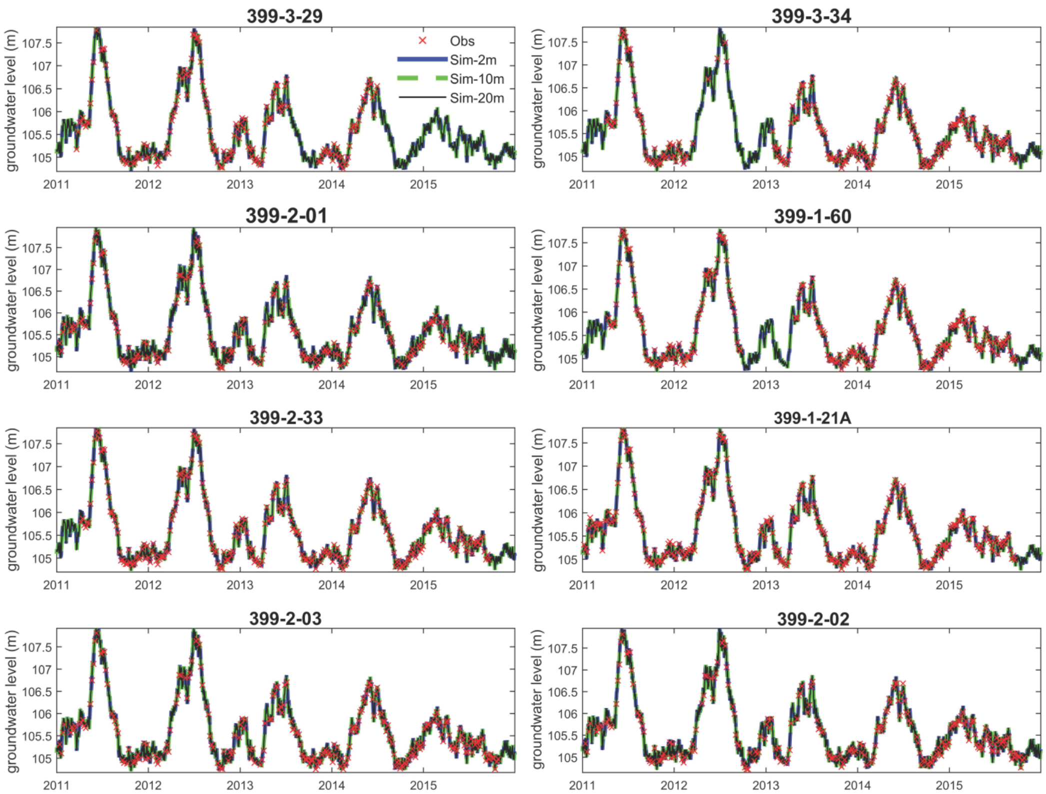

Figure 6. Comparison between simulated and observed water table levels at selected wells shown in the bottom panel of Figure 2.

Geosci. Model Dev. Discuss., doi:10.5194/gmd-2017-35, 2017
Manuscript under review for journal Geosci. Model Dev.
Discussion started: 17 February 2017

Geoscientific Model Development Discussions

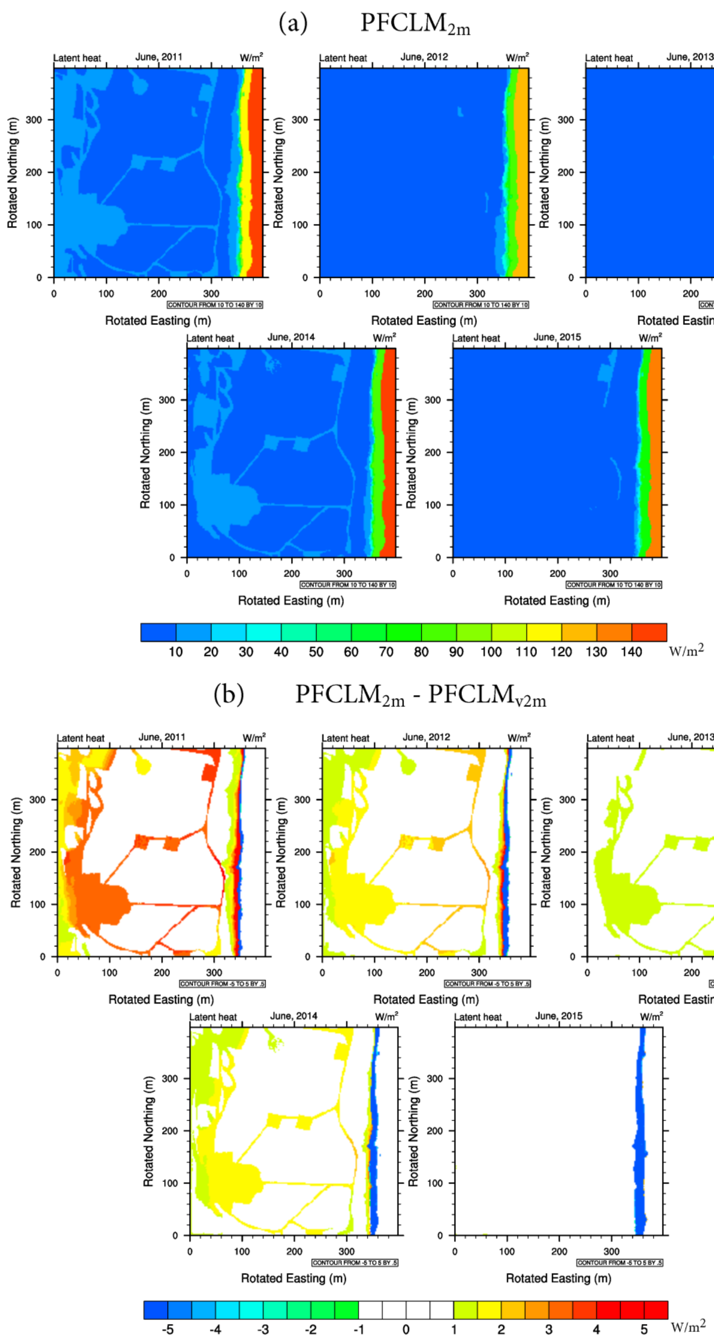

Figure 7. (a) Simulated latent heat fluxes in June from the 3-D simulation ($PFCLM_{2m}$); and (b) the difference between the 3-D and vertical only simulations (i.e., $PFCLM_{2m}$ - $PFCLM_{v2m}$).

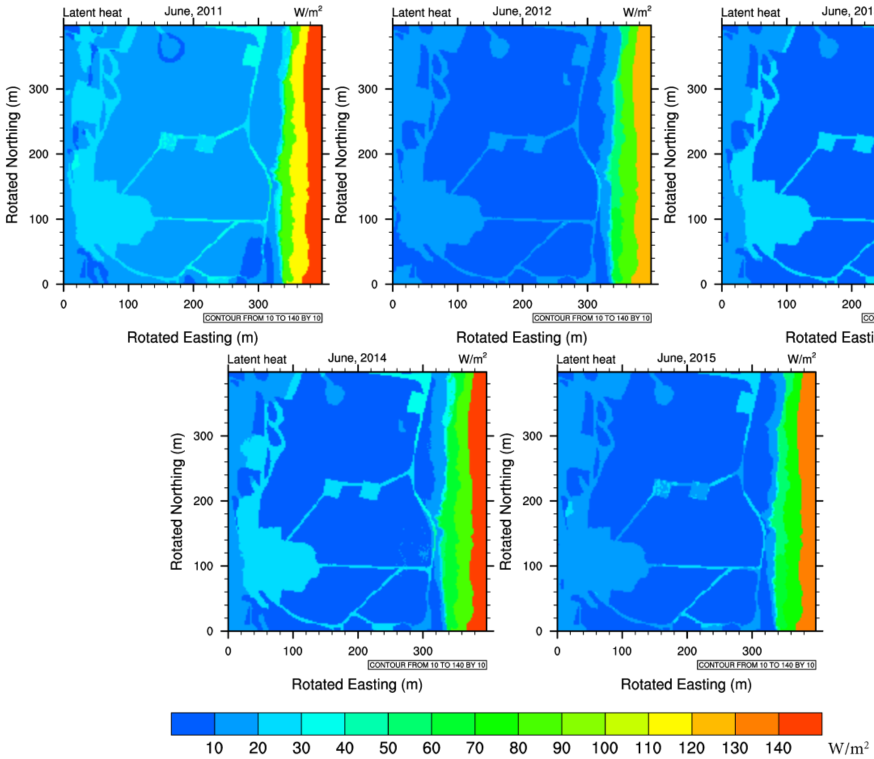

Figure 8. Simulated latent heat fluxes in June from $PFCLM_{E2m}$

Geosci. Model Dev. Discuss., doi:10.5194/gmd-2017-35, 2017
Manuscript under review for journal Geosci. Model Dev.
Discussion started: 17 February 2017

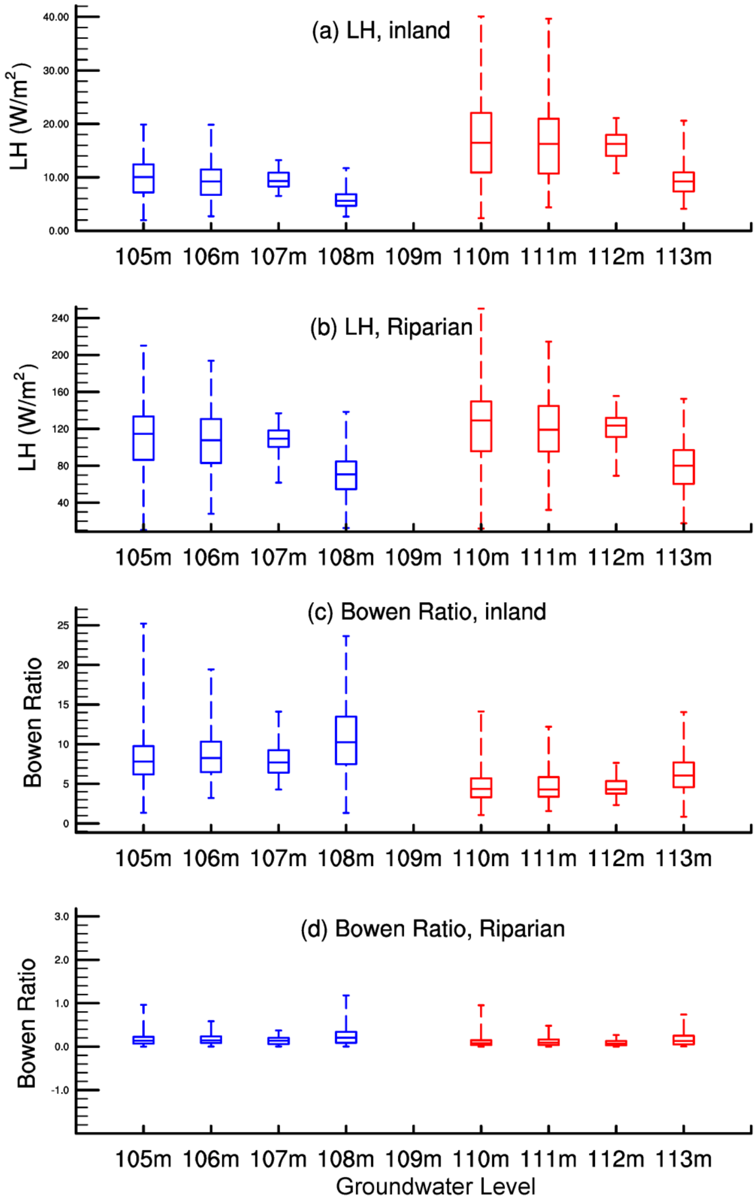

Figure 9. Boxplots of (a) land heat fluxes over the inland domain; (b) and latent heat fluxes in the riparian zone; (c) Bowen ratios over the inland domain; (d) Bowen ratios in the riparian zone in relation to groundwater table levels in the warm month (April to September) in the five-year period. The red boxes and whiskers represent summary statistics from $PFCLM_{2m}$, and red ones indicate those from $PFCLM_{E2m}$. The bottom and top of each box are the 25^{th} and 75^{th} percentile, the band inside the box is median, and the ends of the whiskers are maximum and minimum values, respectively.

Geosci. Model Dev. Discuss., doi:10.5194/gmd-2017-35, 2017
Manuscript under review for journal Geosci. Model Dev.
Discussion started: 17 February 2017

Geoscientific Model Development
Discussions
Open Access

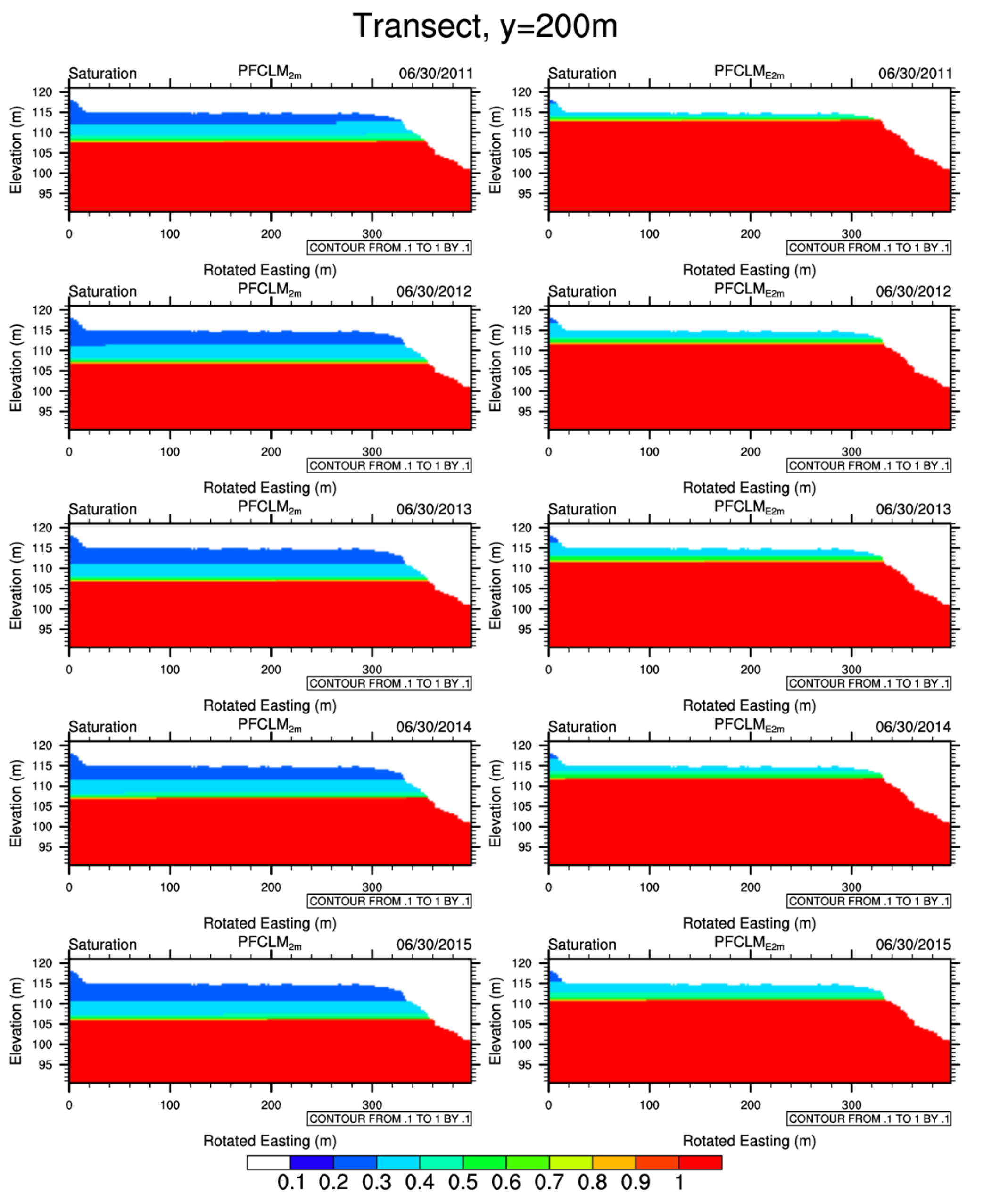

Figure 10. Liquid saturation levels (unitless) across a transect perpendicular to the river (y=200m) on 30 June of each year in the study period from (a) $PFCLM_{2m}$ and (b) $PFCLM_{E2m}$

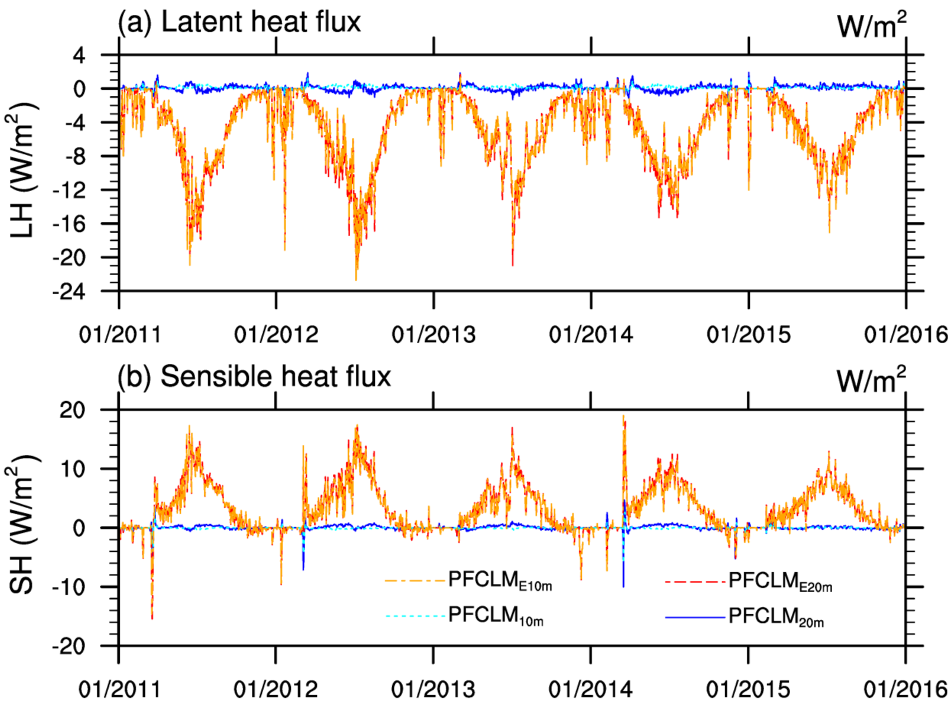

Figure 11. Deviations of simulated domain-average latent heat and sensible heat fluxes from those simulated by $PFCLM_{2m}$ (for $PFCLM_{10m}$ and $PFCLM_{20m}$), and by $PFCLM_{E2m}$ (for $PFCLM_{E10m}$ and $PFCLM_{E20m}$).

Geosci. Model Dev. Discuss., doi:10.5194/gmd-2017-35, 2017
Manuscript under review for journal Geosci. Model Dev.
Discussion started: 17 February 2017

Geoscientific Model Development Discussions

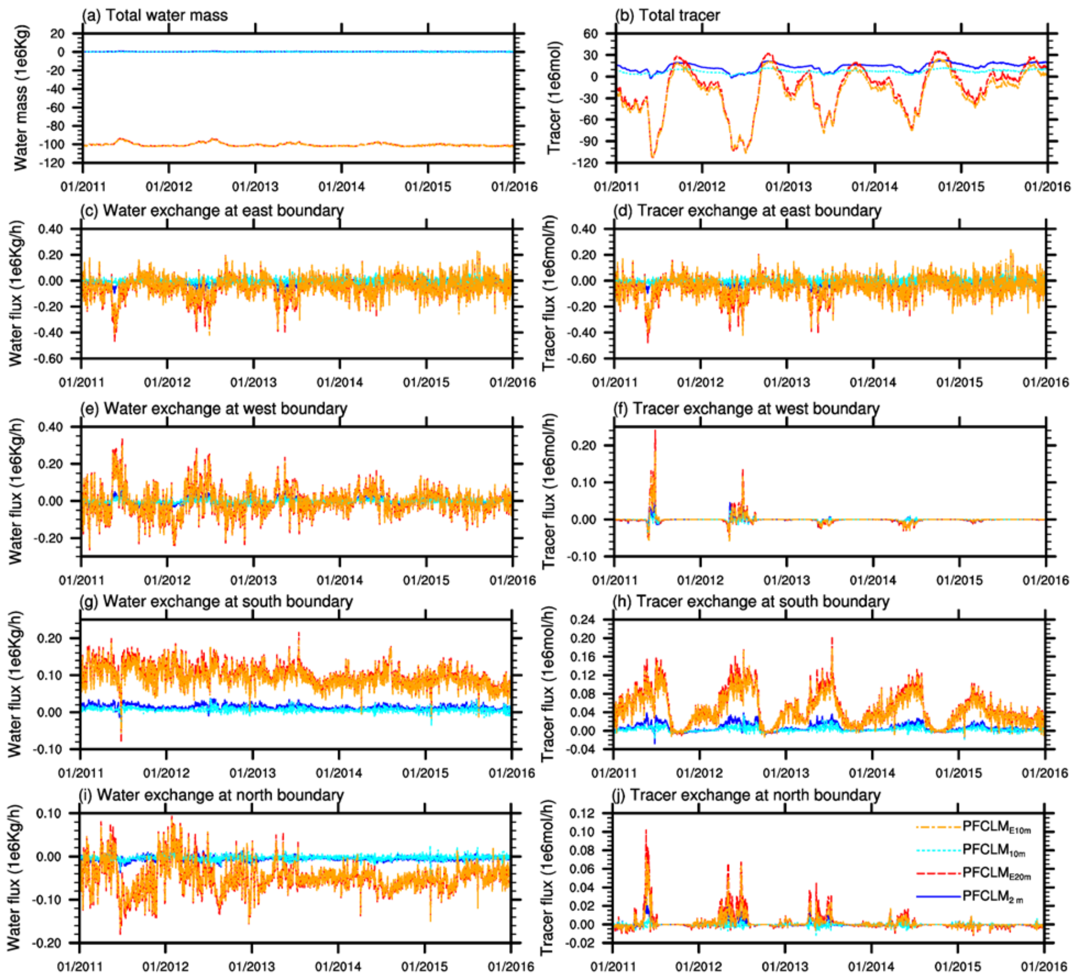

Figure 12. Deviations of total water mass, tracer, and exchange rates of water and tracer at four boundaries from those simulated by PFCLM$_{2m}$ (for PFCLM$_{10m}$ and PFCLM$_{20m}$), and by PFCLM$_{E2m}$ (for PFCLM$_{E10m}$ and PFCLM$_{E20m}$).